Syracuse University

SURFACE

5-2015

Enigmatic rift-parallel, strike-slip faults around Eyjafjörður, Northern Iceland

James Arthur Proett
Syracuse University

Abstract:

Strike-slip faults along mid-ocean ridge and subaerial spreading centers are generally thought to be restricted to transform boundaries connecting rift segments. Faults that are parallel to spreading centers are generally assumed to be normal faults associated with tectonic extension. However, clear evidence of north-south (rift-parallel), strike-slip displacements occur widely around the southern portion of Eyjafjörður, northern Iceland about 50 km west of the actively spreading Northern Rift Zone. The area is south of the southernmost strand (Dalvík Lineament) of the NW-SE-trending, dextral-slip, Tjörnes Fracture Zone (where N-S, sinistral, strike-slip "bookshelf" faulting occurs). Faults in the Eyjafjörður area cut 8.5-10 Ma basaltic crust, parallel to spreading-related dikes, and commonly cut preexisting dike margins. Fault rocks range from fault breccia to gouge. Riedel shears and other kinematic indicators provide unambiguous evidence of shear sense. Most faults show evidence of sinistral, strike-slip movement; less common normal and oblique-slip faults also are present. Cross-cutting relations among the different types of faults are inconsistent thus they are interpreted as being related to a single deformation event. Fault slip-line kinematic analysis yields solutions indicating an overall oblique-slip system with sinistral sense of shear. These results may be interpreted as previously unrecognized transform-fault bookshelf faulting or slip accommodating block rotation associated with northward propagation of the Northern Rift Zone.

Enigmatic rift-parallel, strike-slip faults around Eyjafjörður, Northern Iceland

by:

James Arthur Proett

B.A., Texas A&M University, College Station, TX, 2013

MASTERS THESIS

Submitted in partial fulfillment of the requirements for the degree of

Master of Science in Earth Sciences

Syracuse University

May 2015

Acknowledgments:

I would like to acknowledge the guidance, patience and enthusiasm of my advisor, Dr. Jeffrey Karson, who has played such a huge role in this project and my development as a geologist. I thank my whole committee; Dr. Paul Fitzgerald, Dr. Robert Moucha for all of your patience throughout the writing process. I thank Dr. Paul Fitzgerald for stepping in and being an excellent interim advisor for the first of my masters, for sharing all of you insights on my project as well as whatever you had on your mind it truly made my experience at Syracuse a memorable one. I thank Dr. Bjarni Gautason and ÍSOR for providing me with geologic maps of the area. I thank Keegan Runnals for talking through our similar studies in the office over some darts. I thank all the faculty, staff and fellow students in the department for being so supportive and inclusive during my time here in Syracuse. Finally, I thank my mother and father, for their undying support and guidance throughout my academic career.

Table of Contents

List of Figures

1 Introduction:

The North American-Eurasian divergent plate boundary (Mid-Atlantic Ridge) transects Iceland and makes it an exceptional place to study spreading processes. The subaerial exposure of the spreading system in Iceland is a result of an increased magma budget from the Iceland hotspot. The interaction between the Mid-Atlantic Ridge (MAR) and the hotspot has broad implications for spreading in the region, with the plate boundary being broader and more complexly segmented than in typical mid-ocean ridge spreading centers (Einarsson, 2008). A further complication of the Iceland hotspot is a local eastward offset of the plate boundary zone as it migrates NW relative to the hotspot. The offset is accommodated by transform zones that connect Icelandic rift zones to the Reykjanes and Kolbeisey ridges to the S and N respectively. The hotspot -ridge interaction profoundly complicates the simple model of seafloor spreading, with oblique and segmented rifts, and unstable transforms (Einarsson 2008). Consequently Iceland provides an exciting opportunity to study active subaerial seafloor spreading processes and the deformation associated with it.

Strike-slip faults parallel to rifts are increasingly recognized but interpretation is problematic. In the traditional model of rifting of both oceanic and continental lithosphere, strike-slip faults are generally thought to be restricted to the internal structure of transform boundaries (Gudmundsson and Brynjolfsson, 1993). Parallel to spreading, deformational styles associated with tectonic extension are expected; such as normal faults and fissure swarms (striking perpendicular to the spreading direction). However rift-parallel strike-slip faults have been identified outside of transform fault zones around Iceland (Chutas *et al.*, 2006; Nanfito and Karson, 2009). The presence of these features suggests a previously unrecognized component of rifting in the region. The further understanding of rift-parallel, strike-slip faulting could give insight into the behavior of similar rifts worldwide.

Eyjafjörður in Northern Iceland appears to be a region where rift-parallel strike-slip faulting is

prevalent. The region lies approximately 50 km west of the active N-S trending Northern Rift Zone (NRZ). Southern Eyjafjörður lies outside of any previously identified transform boundary, where rift-parallel strike-slip faults are common, making their presence enigmatic and an excellent location for further study. A kinematic investigation of the area, using quantitative measurements and observations of previously and newly mapped fault zones of the region addresses these issues. Using these data in combination with previous studies, this study presents a refined understanding of the area's deformational history, as well as the tectonic significance of rift-parallel, strike-slip faulting.
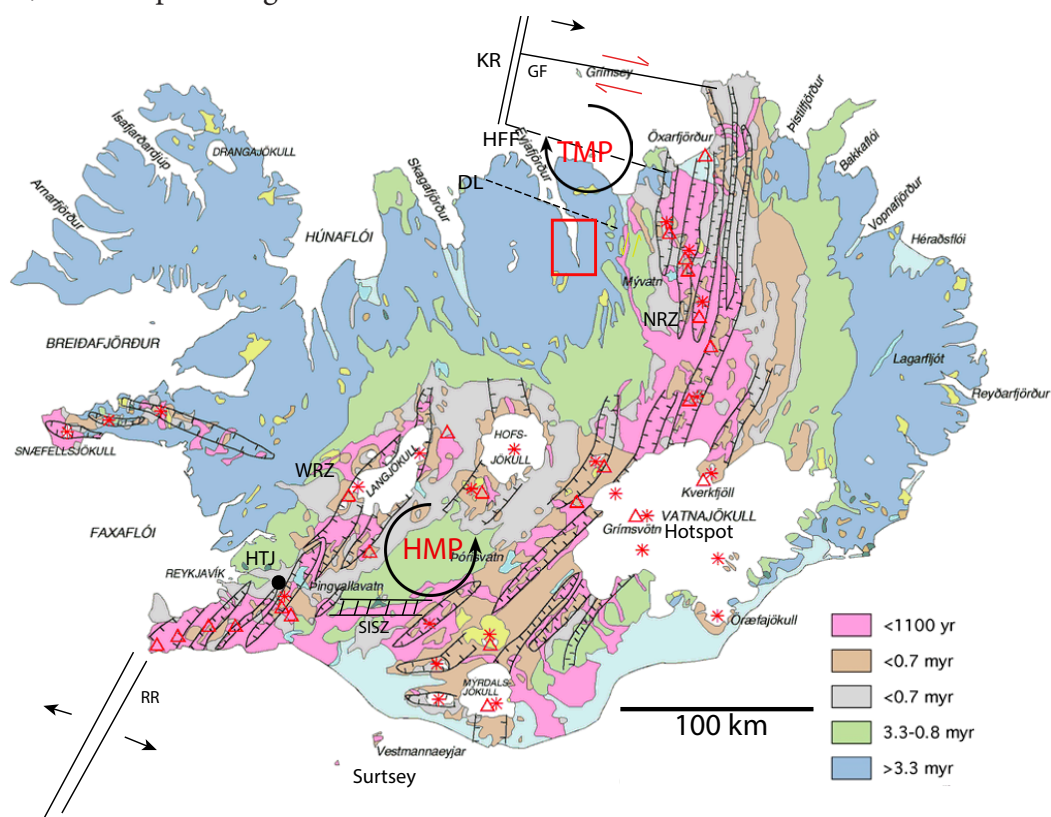
Figure 1. A tectonic map of Iceland that illustrates rift related volcanism and the age of the lavas associated. The red triangles represent active volcanoes, the hashed lines represent fissure swarms, South Iceland Seismic Zone (SISZ), Dalvík Lineament (DL), Husavík-Flatey Fault (HFF), Grímsey Fault (GF), Kolbeinsey Ridge (KR), Reykjanes Ridge (RR), Northern Rift Zone (NRZ), Western Rift Zone (WRZ), Hengill Triple Junction (HTJ). The Hreppar (HMP) and Tjörnes (TMP) mircoplates, with clockwise and counterclockwise rotations respectively, based on the N and S rift propagation (Karson *et al.*, 2011). The focus of this study lies within the red box in South Eyjafjörður, approximately 50 km west of the NRZ (modified from: Jóhannesson and Sæmundsson, 2009).

1.2.Tectonic Background:

Iceland is the subaerial portion of the platform of oceanic crust ranging from ~25-40 km thick (*e.g.* , Einarsson, 2008; Kumar *et al.*, 2007), located on the North Atlantic Ocean. This platform is straddling the Eurasian-North American Plate boundary. Because of its location on an active divergent boundary and above the Iceland Hotspot, the island is a highly active region in terms of both seismicity and volcanism, . Iceland is frequently simplified as a surface expression of the MAR; however it is not as straight forward as that (Einarsson, 2008). The Iceland platform is a unique tectonic setting where rifting and magmatism are strongly influenced by the Iceland Hotspot (which is currently located underneath the Vatnajökull glacier in southeastern Iceland) (figure 1). The plate boundary is clearly defined to the north and south where the MAR intersects the Iceland platform (at the Kolbeisey Ridge to the north and Reykjanes Ridge to the south) (figure 1). Where the plate boundary approaches the Iceland platform, the ridge becomes highly segmented and oblique. In some cases plate motion is even less clear, possibly due to microplates. The mircoplates are small coherent blocks moving independently with respect to the larger plate motion; example the Hreppar and Tjörnes blocks (figure 1) (Einarsson, 2008). The cause of this complicated boundary is a result of the NW migration of the plate boundary relative to the hotspot through time (Bjarnason, 2008). As a result of the NW migration of the plate boundary relative to the hotspot, eastward ridge jumps have occurred maintaining volcanism centered above the hotspot. This eastern jump occurred with the initiation of the Northern Rift Zone NRZ ~7.5 Ma supplanting the western Skagafjörður Paleo-Rift which has been inactive for 3 Ma (*eg.* Hardarson *el al.*, 1997; Garcia *et al.*, 2008). Transform boundaries connect the Eastern Rift Zone to the Kolbeisey and Reykjanes Ridges.

The Iceland hot spot in the NE Atlantic, straddles the spreading center in eastern Iceland . This results in the roughly symmetrical magmatic "trail" of the hotspot, on either side of the spreading center. The "trail" is created by excess hotspot-related magmatism resulting in a bathymetric high on the sea floor. These hotspot trails can be traced eastward from large plateaus of flood basalts

on the eastern coast of Greenland on the North American Plate defining the ridge to the east (Greenland-Iceland ridge to the west and the Faeroe-Iceland Ridge to the east). These patterns of magmatism indicate that the Iceland hotspot is at least as old as the opening of the North Atlantic at ~55 Ma, are determined from magnetic anomalies (Bjarnason, 2008). However the hotspot is possibly as old as 130 Ma, with evidence of the track passing from west to east Greenland (Lawyer and Müller, 2006). The center of the Iceland hotspot currently is the highest topographic feature in the island lying beneath the Vatnajökull glacier. It is also a major driver in the rift propagation and volcanism in the region.

The MAR approaches Iceland from the SW as the Reykjanes Ridge. The Reykjanes Ridge becomes increasingly oblique to the plate motion direction as it approaches Iceland and begins to resemble a much faster spreading system, seismically and topographically (Einarsson, 2008). This obliquity, seismicity and topography of the ridge can be attributed to its proximity to the Iceland Hotspot
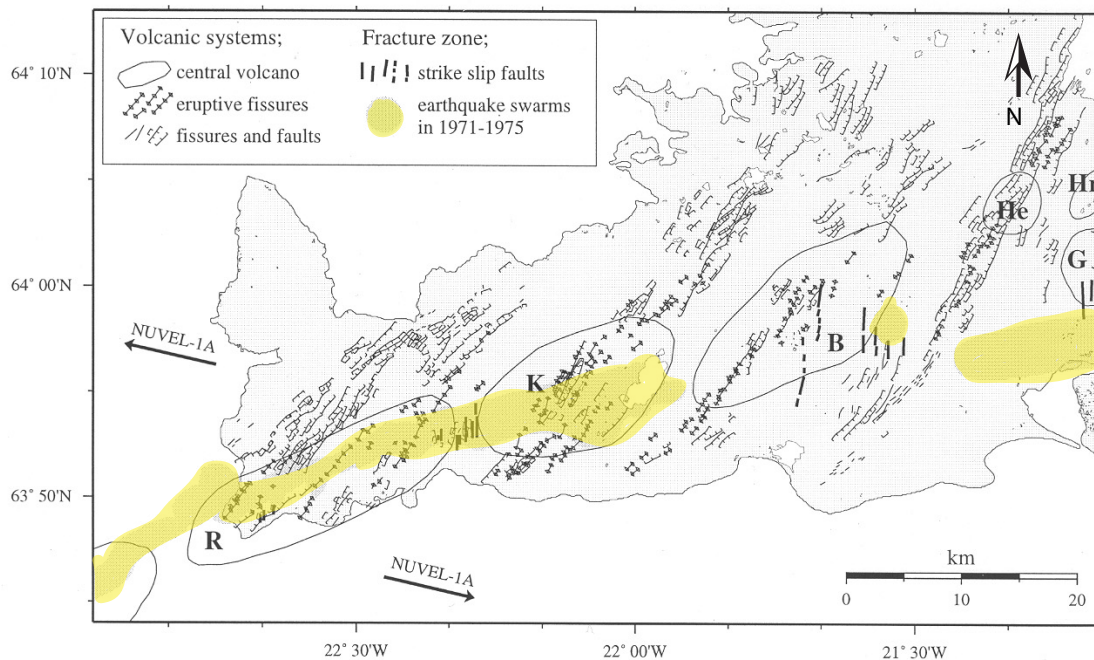
Figure 2. Faults and fissures (black) on the Reykjanes Peninsula are oblique to the overall trend of the plate boundary zone (yellow). Arrows show plate motions directions from models NUVEL-1A and NUVEL-1A (modified from LaFemina *et al.*, 2005).
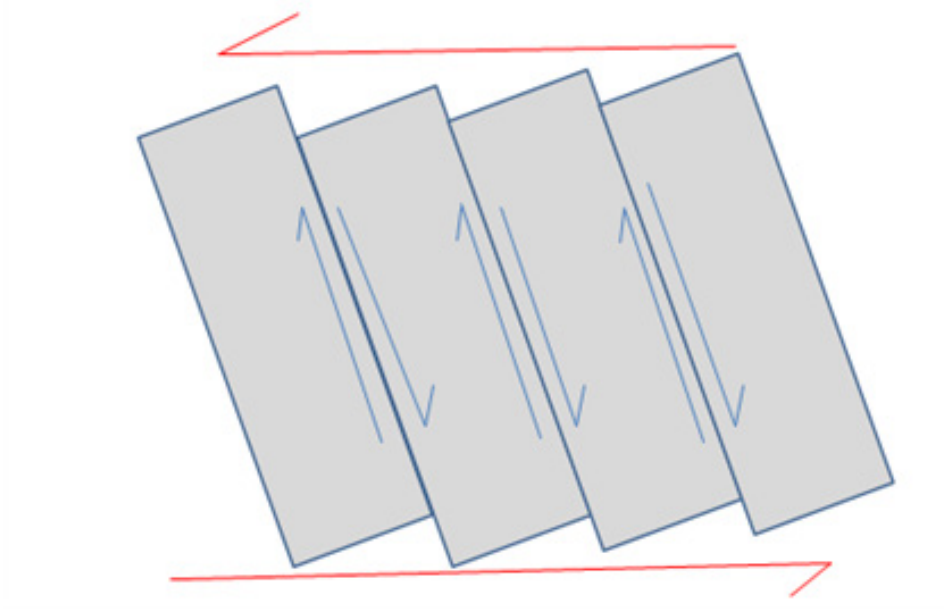
Figure 3. An idealized model of bookshelf faulting. For an overall sinistral-slip transform zone (such as the South Iceland Seismic Zone), slip is accommodated by *en echelon* dextral strike-slip faults, striking at a high angle to the overall transform trend.

(Einarsson, 2008). The Reykjanes Ridge runs onshore at the Reykjanes Peninsula on the SW tip of Iceland where the ridge becomes highly oblique trending 070° up the length of the peninsula (figure 2) and has a spreading rate of ~20 mm/a in the 105° direction (LaFemina *et al.*, 2005). The plate boundary along the Reykjanes Peninsula is characterized by a series of *en echelon* volcanic shields and fissure swarms. These features are cut by normal faults and eruptive fissures that are initiated by laterally propagating dikes along the ridge axis from a central volcano. The trend of these dikes are ~350° which is highly oblique to the plate boundary and spreading direction (Einarsson, 2008). In this part of the plate boundary, magmatism is episodic and the mechanism by which strain is accomplished is dependent on magmatic activity. In order to accommodate offsets between volcanic systems there are a series of NS-trending strike-slip faults in a 'dry' magmatic period, while in a "wet" period strain is accommodated by dike injection and fissure eruptions. These features are observed northeast along the Reykjanes Peninsula until the ridge hits the Hengill Triple Junction. At the eastern terminus of the Reykjanes Ridge, some spreading

continues to the north in the dying branch of the Western Rift Zone (WRZ) (figure 1). According to GPS measurements, the WRZ only currently accommodates ~15% of spreading (LaFemina *et al.*, 2005). Due to the NW motion of the plate boundary, relative to the location of the hotspot, the ridge has experienced a large right step (in the direction of the Iceland hotspot). In essence the location of the hotspot focuses the plate boundary to the east of the regional N-S trend of the MAR. This right step in the plate boundary, from the Reykjanes Ridge (at Hengill Triple Junction to the more active Eastern Rift Zone (ERZ) is accommodated by an E-W transform zone (figure 1). The transform region is called the South Iceland Seismic Zone (SISZ) and is associated with frequent earthquake activity. The SISZ has an overall left lateral motion that is accommodated by parallel N-S strike-slip faults that have a right-lateral sense of motion (figure 3). This style of faulting is known as "bookshelf faulting" and is prevalent in the migrating transform regions of Iceland. The SISZ is the most seismically active region in Iceland with mapped and surficially defined dextral-slip strike-slip faults oriented ~N-S.
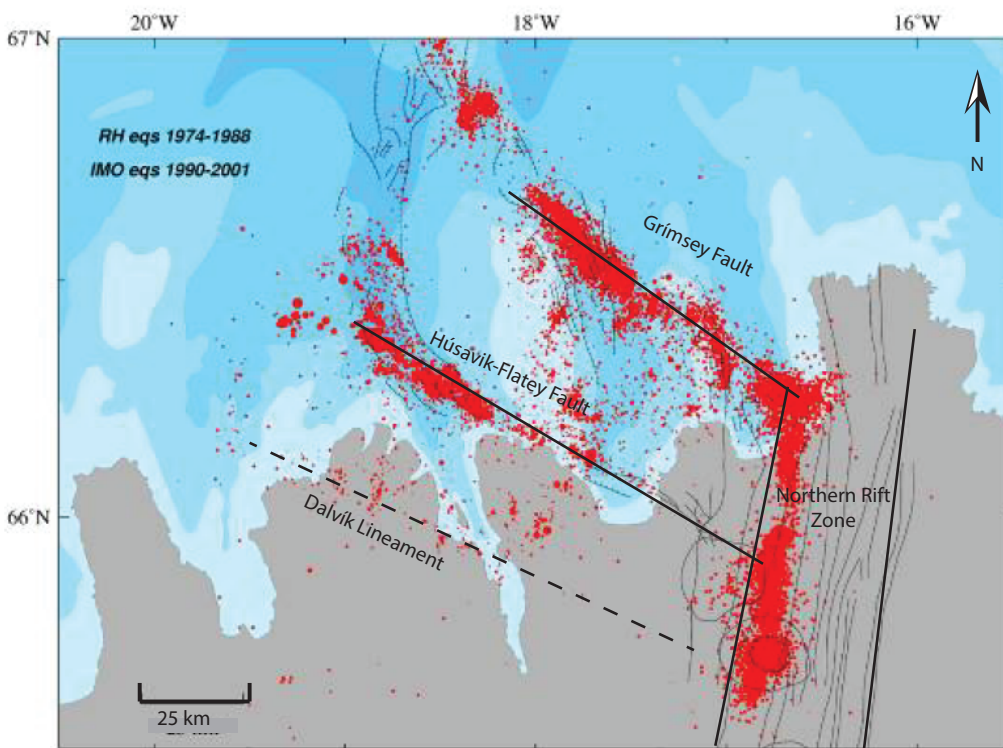
Figure 4. Seismisity of the Tjörness Fracture Zone (1974-2001) (modified from Sæmundsson and Karson, 2006).

The SISZ intersects the Eastern Volcanic Zone (EVZ) to the east at a triple junction. The ERZ extends northward through the hotspot (under the Vatnajökull glacier). Spreading propagates away from the hotspot terminates to the southwest at the island of Surtsey (Karson *et al.*, 2013; LaFemina *et al.*, 2005) (figure 4). This rift propagation can be results in what is termed in the literature as "pseudofaults" (Hey, 1977); a discontinuity in age of crust between laterally adjacent rock units associated with rift volcanism or formation of new oceanic crust. The spreading rate is greatest at the Iceland Hotspot (19.8mm/a), and decreases to the SW because of overlapping of the WRZ and ERZ (LaFemina *et al.*, 2005). This area is the most active volcanic region in Iceland and is the location of Eyafjallajökull, well known for its 2010 eruption that disrupted air travel throughout Europe and across the Atlantic Ocean. The ERZ has taken over as the dominant spreading center in south Iceland over the past 3 Ma currently accounting for ~85% of plate motion relative to the dying WRZ (LaFemina *et al.*, 2005). Features in this area are normal faults and fissure swarms that generally strike parallel to the rift zone (Einarsson, 2008). However, a much of this region is currently covered by glacial ice obscuring the details of the rift structure.

The Northern Rift Zone (NRZ) lies on the north side of the hotspot. Similar to the ERZ the NRZ propagates northward from the hotspot creating V-shaped pattern defined by pseudofaults to the east and west the rift zone (Einarsson, 2008; Karson *et al.*, 2011). Also analogous to the ERZ the spreading rate is greatest near the hotspot with a rate of 19.4 mm/a (LaFemina *et al.*, 2005). At the propagation tip (and down the western limb of the NRZ) the rift is connected to the MAR segment (the Kolbeinsey Ridge) offshore to the north by a left-stepping transform system (Tjörnes Fracture Zone (TFZ)). Lava shields in the NRZ mark central volcanic system and the rift zones are defined by their generally N-S trending fissure swarms and extensional features such as normal faulting. The NRZ is a volcanically active region with episodic volcanism. In the past thousand years the most active volcanic systems are centered on the Krafla and Askja central volcanoes. The recent Krafla Fires eruptions in the 1970's and 1980's caused massive 9 m inflation

of crustal deformation along the rift zone at the northern extent of the NRZ (Einarsson, 2008).

The TFZ links the Kolbeinsey Ridge (in the west) to the NRZ (in the east) as a left-stepping transform system analogous to an SISZ. The TFZ is composed of three fault strands that trend ~WNW, (figure 5). These are the right-lateral fault systems whose strain is accommodated by WNW strike-slip faults bounding areas with sub-parallel left-lateral strike-slip faults striking NNE (Young *et al.*, 1984; Karson *et al.*, 2013). As the NRZ has propagated north through time, the transform system has migrated north along with the rift, leaving a band of onshore crustal deformation on the Tjörnes and Flateyjarskagi Peninsulas in NE Iceland. Transform fault strands have become abandoned as the system migrates northward, but these strands are seismically active. This conclusion was drawn based on the decreased seismic activity of the fault strands to the south (Brandsdóttir *et al.*, 2004). The currently most seismically active strand is the Grímsey Fault (GF), the farthest north of the known segments, that connects to the Kolbeinsey Ridge and the Krafla volcanic complex. The middle of the three strands, the Húsavik-Flatey Fault (HFF), has intermediate seismic activity both on and offshore Iceland. The farthest south strand of the TFZ (~30 km south of Húsavik) is the Dalvík Lineament, a far less seismically active region with little surface expression of fault related deformation (Brandsdóttir *et al.*, 2004; Einarsson, 2008; Karson *et al.*, 2013). As the transforms linking the two systems migrate north the Kolbeinsey Ridge has become abandoned south of the active linkage in the GF as the NRZ has taken over spreading. The HHF and the Dalvík Lineament are connected to the dying Eyjafjarðaráll Rift which is the former southern extension of the Kolbeinsey Rift (Einarsson, 2008).
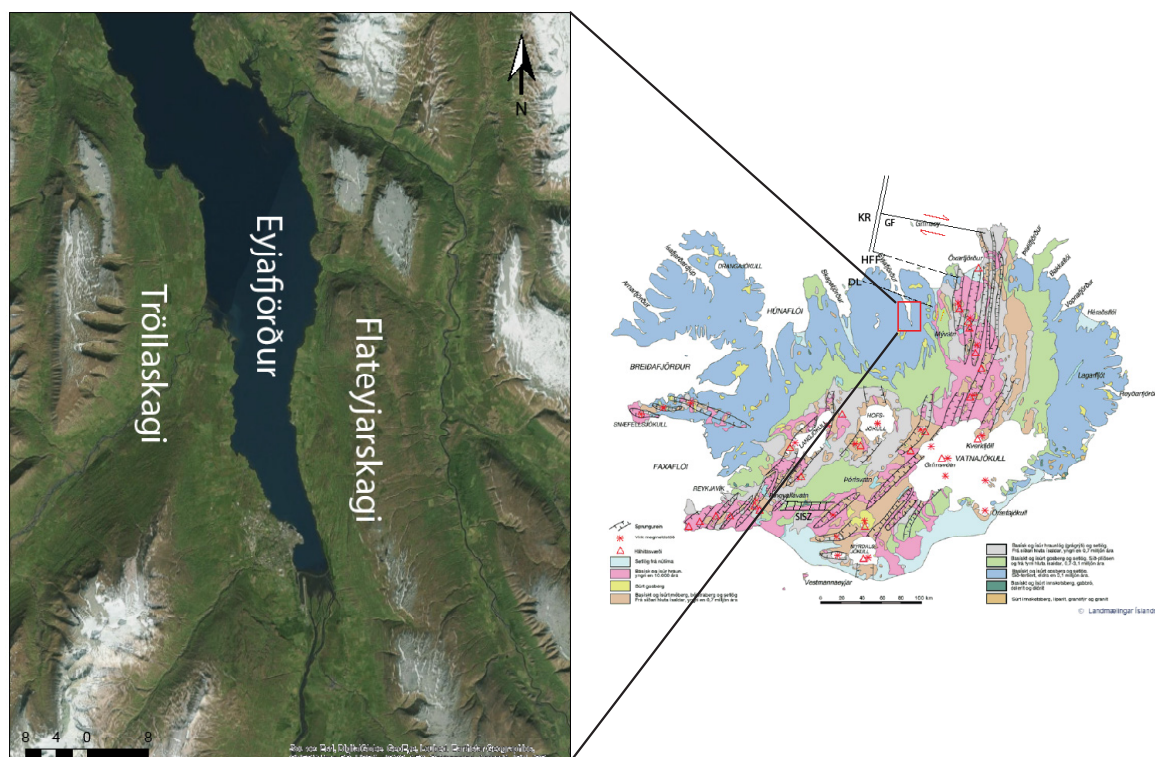
Figure 5. A satellite image of the study area is shown (left). The southern parts of the two peninsulas, Tröllaskagi, to the west and Flateyjarskagi to the east, are separated by Eyjafjörður. The tectonic map (right) shows the study area in a regional and tectonic context (modified from: Jóhannesson and Sæmundsson, 2009).

1.3 Study Area:

The area investigated in this study focuses around the southern portion of Eyjafjörður. Eyjafjörður is the longest fjord in Iceland and is bound by Flateyjarskagi to the east and Tröllaskagi to the west. This area is in a ~50 km long by ~30 km wide region, located about 50 km west of the NRZ. The area is just south of the southernmost strand (Dalvík Lineament) of the NW-SE-trending, dextral-slip, Tjörnes Fracture Zone, where N-S, sinistral, strike-slip "bookshelf" faulting occurs. The geology of the region is dominated by 10-5 Ma tholeiitic flood basalts, tilted eastwards with increasing dip to define a "flexure zone" (Young *et al.*, 1984). These lavas dip approx. 0°-20° to the ESE; toward the active NRZ (Jancin, 2010). Faulting along Eyjafjörður is well documented north of the Dalvík Lineament; however data south of the TFZ are much more limited. Current geologic maps of the area provided by the Iceland GeoSurvey (ÍSOR) display

NNE-striking subparallel normal faults. Further investigation of this area suggests that this is a oversimplification. Normal, oblique and strike-slip faults are abundant throughout this area and all seem to strike roughly parallel to the NRZ, that is N-S.

Fault zones are best exposed along the east coast of Eyjafjörður as well in road cuts where relatively fresh sections are visible. Stream cuts also trending ~E-W through the cliffs' that define the fjord on either side, providing cross sections perpendicular to the strike of many of these tectonic features. The western side of the fjord (South Tröllaskagi) is marked by an extensive cover of glacial sediments, obscuring the basement geology; however, the exposed section in this area does not appear to have undergone the same extent of deformation as on Flateyjarskagi to the north and east.

The presence of hydrothermal vents in Eyjafjörður is quite extensive and consists of series of vents and fissures that stretch hundreds of meters along the sea floor (Reed, 2006). Hydrothermal activity is not limited to the fjord as numerous hot springs are observed on land throughout the region. These hydrothermal systems have been quite disruptive; recent attempts to tunnel from through the Vaðlaheiði mountain's lavas (just E of Akureyri) ran into major problems when it hit a hydrothermal system in early 2014, expelling hundreds of liters per second of over 50° C water.

1.4. Previous Work:

Several previous studies have been undertaken in northern Eyjafjörður (north of the Dalvík Lineament), detailed investigations of southern Eyjafjörður are limited. In particular deformation in southern Eyjafjörður has been highly generalized and mentioned only peripherally with respect to the Dalvík Lineament. Studies of the Tjörness Fracture Zone to the north suggest that southern Eyjafjörður is an area characterized by only widely spaced normal faults and dikes, striking perpendicular to spreading direction (Gudmundsson and Brynjolfsson, 1993; Jancin, 2010; Young

ORKUSTOFNUN
RANNSÓKNASVIÐ

Svalbarðseyri

Eyrarland

Svalbarðseyri

Breiðabó

(órsnes)

Krossanes

Krossanes

Litlihvamm

(Sólheim

Höfð

AKUREYRI

A

POLLURINN

Fífilbrekka

aðar

Leiran

Vaðlaland

VAÐLAHEIÐI

VADARA

Vesti

Nes

Finuska

A'

VAÐLAHEIÐI
Jarðfræðikort/Geological map

	Þykk laus setlög / *Thick sediments*	Misgengi og brot / *Faults*
oo	Dyngjubasalt í Bíldsskarði(N) / *Compound lavas*	Berggangur / *Dyke*
dd	Dílabasalt (R) / *Porphyritic basalt*	Strik og halli / *Strike and dip*
set	Setlagasyrpa, mislægi? / *Sedimentary horizon*	Borhola / *Borhole*
fí1	Finnastaðadalssyrpa (N/R) / *Finnsstaðadalurtholeiite*	Þversnið / *Section*
hr4	Stórharnarsdílabasalt (R/N) / *Stórhamar porphyritic basalt*	
hr3	Blönduð basaltsyrpa (N) / *Mixed basalt layers*	
dy3	Bíldsárdyngja (dílótt) (R) / *Bíldsá compound olivine basalt*	
dy2	Brókárdyngja (dílótt) (N) / *Bróká compound olivine basalt*	
hí1	Heimari-Lambársyrpa, þóleiít (N) / *Tholeiite*	
va4	Vatnsbólaþóleiít (R/A) / *Tholeiite*	
va3	Vatnsbólaset, sandsteinn / *Gilsá sandstone*	
va2	Vatnsbóladílabasalt (A) / *Wells porphyritic basalt*	
av6	þóleiít (N) / *Tholeiite*	
av5	Dílabasalt (N) / *Porphyritic basalt*	
av4	þóleiít (N) / *Tholeiite*	

Tilvísun í kortið/Referer to this map as:
Árni Hjartarson 2001:
Vaðlaheiði, jarðfræðikort.
Orkustofnun, Reykjavík.

Hæðarlínubil er 5 m (nema austast á
kortinu þar sem það er 20 m)
Keiluvörpun, viðmiðun ISN93
Unnið í landfræðilegu upplýsingakerfi
(Arc/Info®).
Kortgrunnur er byggður á hæðarlínum frá
Loftmyndum ehf sem gerðar eru eftir
flugmyndum frá 1998 of 1999.
© Orkustofnun, Reykjavík

1:25.000

Þversnið um Vaðlaheiði
Kvarði: lóðrétt/lárétt = 1/5

A

A'

Svalbarðsströnd

Fnjóskadalur

(m)

800
600
400
200
0

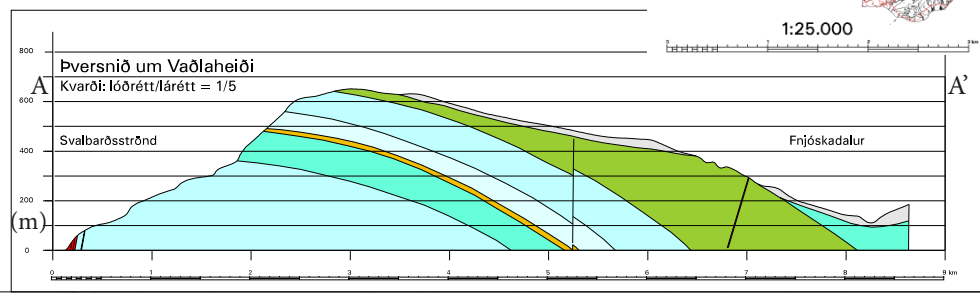0   1   2   3   4   5   6   7   8   9 km

Figure 6. A 2001 geologic map of the region provided by the ÍSOR (Iceland Geosurvey). The structural features on this map are entirely extensional features: Dikes and normal faults. The NE-SW cross-section (red line) from A-A' reveals 7 units of variable thickness dipping gently to the east (toward the NRZ). (Hjatarson, 2001)

et al., 1985). A theoretical paleostress model by Långback and Gudmunsson, (1995) suggested a possible sinistral strike-slip component associated with the Dalvík Lineament. This investigation reported minor sinistral strike-slip faults directly south of the liniment on the Tröllaskagi Peninsula, but considered this case to be anomalous. The area has been mapped by the Iceland Geosurvey (ÍSOR) shown in Figure 6. The offsets of gently dipping map unit contacts indicate at least some vertical separation on the faults, but additional kinematic data is not reported.

2. Methods:

In order to accomplish the objectives of this study faults were identified, mapped and analyzed based on their attributes. Fault zone outcrops range from meter to kilometer scales and are evaluated based on their atributes (dike and fault surfaces are where their kinematic properties can be best assessed). The largest and best exposed features are typically concentrated along the Eyjafjörður shoreline (roughly parallel to their strike). Steep, incised stream cuts orientated roughly perpendicular to strike, provided excellent E-W transects, adding a three-dimensional perspective to the study.
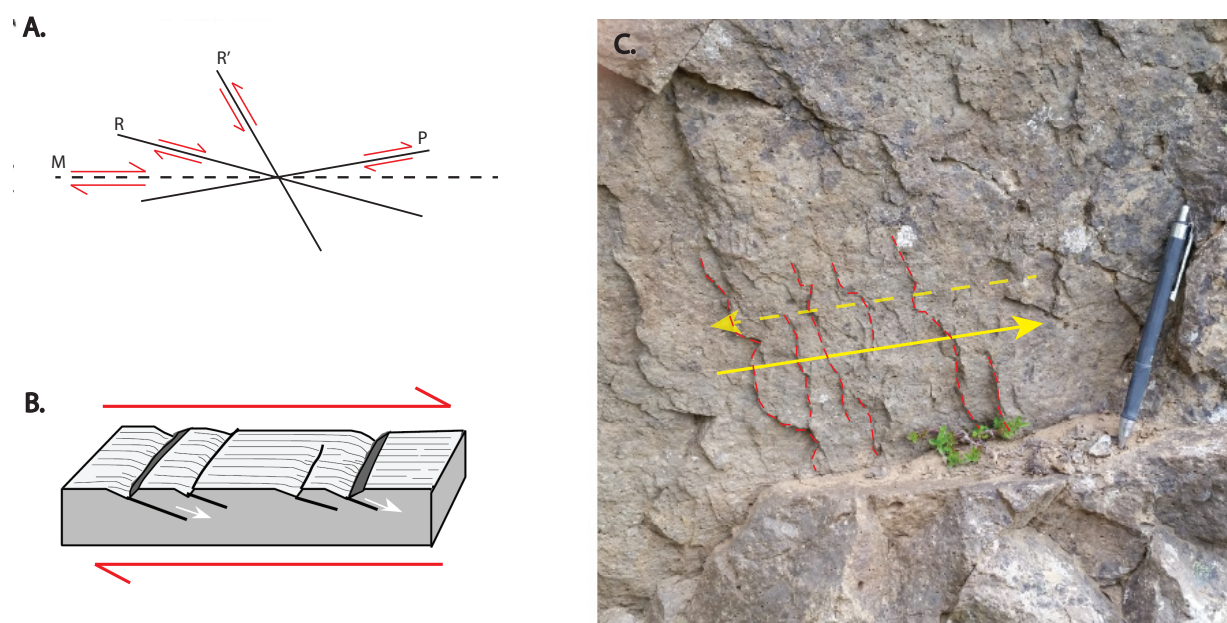
Figure 7. Interpretation of fault-slip data in the field. **A**. Preferred orientations of fractures: the dashed line, M represents a sinistral slip fault, R, Riedel shears (synthetic slip) ~15° from the fault surface, R' represents anti-Riedel shear (antithetic slip) ~75° from the fault surface, P shears (synthetic slip) ~10° from (Petit, 1987). **B.** Schematic example of Reidel shears and sense interpretation (red half arrows) (Petit, 1987). **C.** Riedel shears in a photo from subarea #2 denoted by red dashed lines.

The data collection preformed at these fault zones include: preliminary investigation by aerial photograph their specific location (measured with hand held GPS), the strike and dip of the faults, rake of the slickenlines, dike orientations and thickness, vertical offsets, damage zone and gouge characteristics and any other relevant observations of the fault zone. The slip sense of these faults was determined by the presence of small-scale shear fractures (most notably Riedel shears) (Petit, 1987) (figure 7). These synthetic shear fractures are quite prominent and recognizable across a range of scales from cm to tens of meters. Representative samples of fault rocks were in some cases collected for further study. Unfortunately all samples of fault breccia, became increasingly friable as they dried and to fragile for further study, however more coherent samples provide excellent information about the micro-structures and petrology of these fault rocks.

Individual fault orientations are analyzed for strain and kinematics using strike, dip and rake, presented according to the Aki Richards format (Marrett & Allmendinger, 1990) and utilizing FaultKin kinematic software (Allmendinger, 2012). All fault measurements are plotted with respect to their principal axes of strain, where P represents maximum shortening direction and T represents maximum extension direction. These principal axes lie 45° from the pole of the fault plane (figure 8A and 8B). A total population of P and T-axises is complied and contoured based on statistically significant concentrations and divided into quadrants based on their distribution. These P and T quadrants are then used to generate strain diagrams, analogous to earthquake focal mechanisms (figure 8C; Marrett & Allmendinger, 1990).
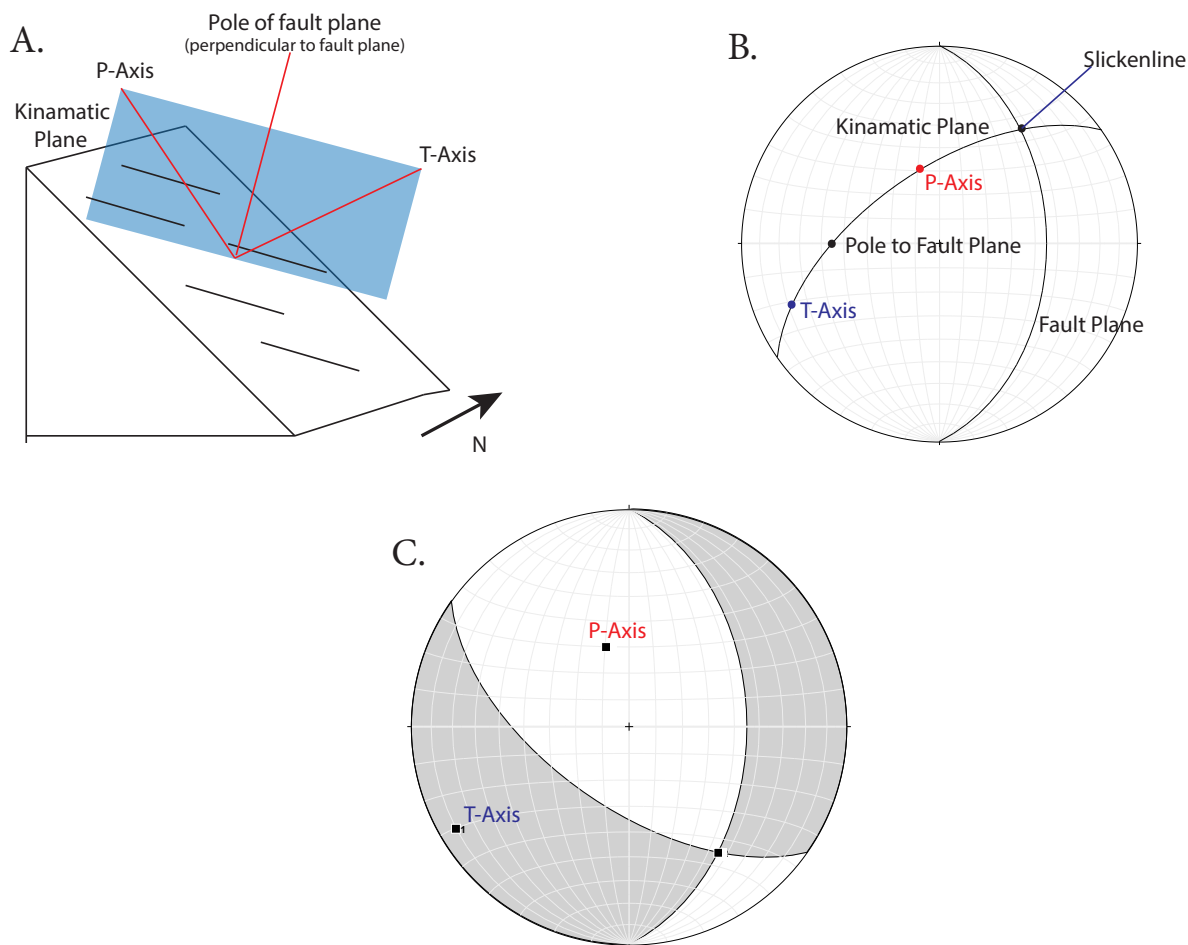
Figure 8. A,B. Orientations of features and movements appear on both A and B diagrams; A fault plane striking N-S, dipping 45° W, slickenlines plunging 45° N (indicators of normal-slip). The kinematic plane (blue rectangle) defined by striae and normal to the fault plane 45° to either side of the pole in the fault plane lie the P (shortening), T(extension) axis where the maximum principal directions of strain are located and lie in the kinematic plane. **C.** A population of these P axes and T axes are compiled and the nodal plane is estimated segregating the P-T axises. The P/shortening quadrants is shaded (Allmendinger, 1989).

3. Field Observations and Results:

3.1 Rock Units:

Exposed lavas in the area are primarily Upper Miocene to Lower Pliocene theolitic flood basalts (Jancin, 2010). The stratigraphy of the area is marked by lava flows ~10 m thick, separated by vesicular flow-tops and thin inter-basaltic sediment layers ranging in thickness from a few centimeters to 1.5 m. The thin sediment layers have been baked by the overriding lava flows giving them an altered, reddish-brown hue (figure 10)(Kristjansson *et al.*, 2004). The basal contact between flows is generally more sharp. The top of most of the flows are commonly marked with vesicular basalts and scorias or flow top breccias (figure 9). The lower flow units are generally tabular, cliff forming units. Lower unites frequently display columnar joints. Flow top breccias are less coherent units, typically friable and altered. As a result structures are difficult to decipher in these flow top units.

Figure 9. A flow-top breccia (slope former) grading upward into a tabular lava flow (cliff forming unit). The white dotted line marks the upper boundary of the flow top unit.
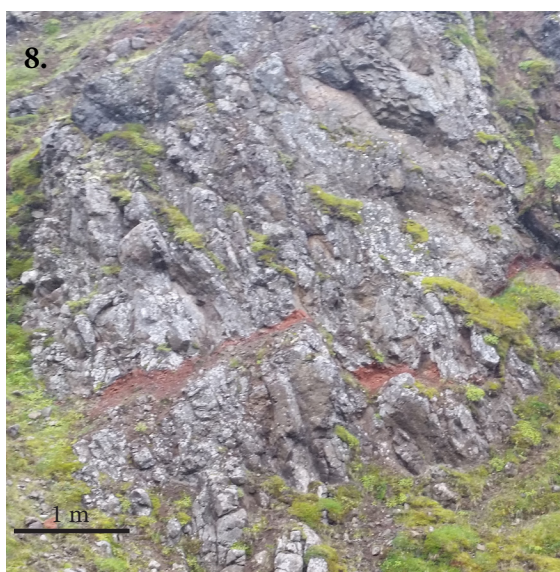
Figure 10. The thin undulating red bed (offset by small fault) is an example of a baked sediment layer between two flows.

In general, the lavas strike ~350° and dip $0°$-$10°$ to the E, toward the northern part of the map area on both the Flateyjarskagi and Tröllaskagi. In the southern part of the map area, the lava dip changes to a southerly direction (striking ~080$°$). The dip angle remains fairly constant on the Tröllaskagi (~0$°$-10$°$) side however, dips is as steep as 15$°$ in southern Flateyjarskagi. The increased dip angle in southern Flateyjarskagi is possibly due to the presence of a large NNE-trending flexure zone which cuts throughout the area (figure 10) (Garcia *et al.*, 2006).

3.2 Dikes:

The surrounding lava flows and dikes have a similar composition to the lava flows, of tholeiitic

Figure 11. A fractured dike margin (shown in blue) related to faulting in sub-area 5. (figure 13)

Figure 12. A heavily fractured dike (yellow dashed lines) cut by a fault (red deashed lines)in subarea 15. (figure 13)

basalt (Kristjansson *et al.*, 2004). Dikes in the area are generally trend N-S and vary mostly from 345°-015°. Individual as well as composite dikes are present. Individual dikes ranged in thickness from 25 cm to 4 m. The orientation of dikes in the region is variable: NE, dip of dikes are vertical to nearly vertical 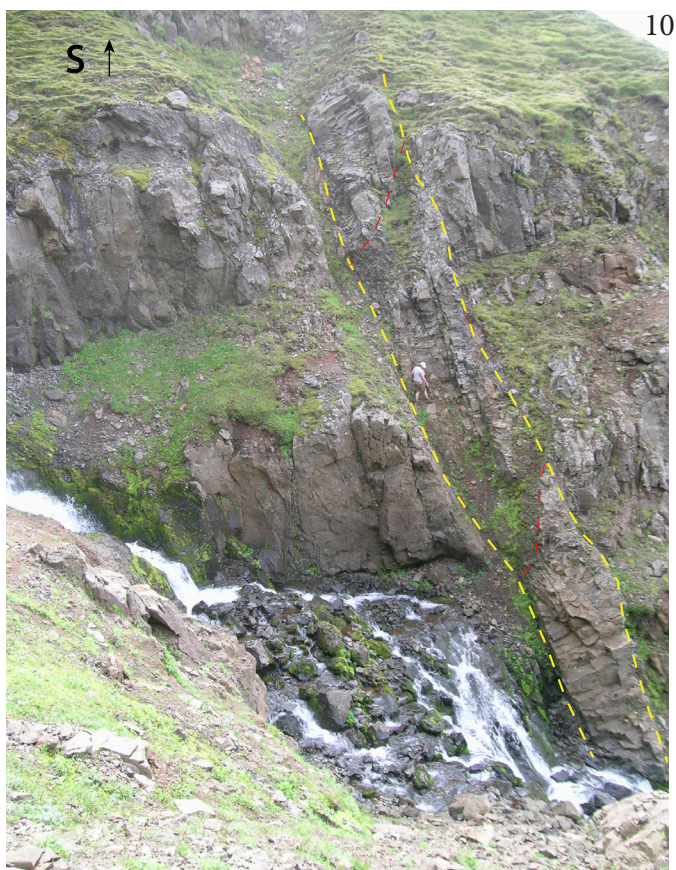and strike 355°; the SW, dip 65°-70° to the west and strike 345°-015°; the SE, dip 80° to the west and strike 015°; NW, dip vertical to nearly vertical and strike 000° (figure 12). The dip of the dikes appears to be almost perpendicular to flows in all locations, suggesting that they were intruded through flat-lying lava flows and later tilted (figure 10). Dikes are cut by both normal and strike slip-faults. No clear correlation between dike deformation and style of faulting was evident, however dike intrusion and tilting predates the fault deformation. Both normal and strike-slip faults occur in close proximity to one other and to both be preferentially focused along preexisting dike margins.

3.3. Fault Zones:

Fault zones are characterized by damage zones in surrounding rocks and closely spaced shear & extension fractures and joints. Fault cores have cataclastite and minimal gouge (figure 13). These damaged zones ranged in thickness from ~1 m up to 100 meters. Zeolites are comman within void spaces created by fault related fractures; the most common of which are scolecite ($CaAl_2Si_3O\cdot3H2O$) and stilbite ($NaCa_4(Si_{27}Al_9)O_{72}\cdot28(H_2O)$) (Sæmundsson and Gunnlaugsson, 2002). Polished and striated fault surfaces occur and are coated with syn-kinematic mineralization. The mineralogy of these coated surfaces is predominantly quartz and calcite that formed as either the result of syn-kinematic crystallization or deposition by fluids (Passerini *et al.*, 1997). A less common brown mineralized surface composed of clay minerals and iron oxide occurs in one locality in the SW of the map area. This brown surface is associated with strike-slip faults throughout Iceland (Passerini *et al.*, 1997).

Fault-related striations occur on fault surfaces as slickenlines (abrasional marks) or slickenfibers (linear crystal growths) (figure 14). Typically these striae are particularly well preserved on

freshly exposed surfaces, such as along the shore or road cuts. The orientations of slickenlines varies by location. Locally horizontal striae occur in close proximity to surfaces with vertical striae. In some areas fault surfaces and slickenlines have similar orientations with gently plunging slickenlines on steeply dipping fault surfaces. Although diverse orientations of striae are typical of outcrops in southern Eyjafjörður.

Figure 14. A mineralized faults surface with well preserved slickenfibers (near horizontal).

Figure 13. Highly fractured fault zone core with cataclastite fault rocks (rock hammer for scale).

Figure 15. A map of the study area, with dike and fault plane orientations. The fault trends are grouped by subareas with similar fault geometries and geographic proximity. Dikes: red (this study) and yellow ÌSOR - Hjatarson and Harðardóttir, 2004; Hjatarson and Jónsdóttir 2004; Hjatarson, 2001).

3.4. Fault Kinematics:

The trends of structures in the region have a bimodal distribution (figures 15 and 16). The dominant orientation of fault and dikes are either NNE and NW (220/261 faults) (figure 15). Faults in both NNE and NW orientations are predominantly sinistral strike-slip and oblique faults. The major exception to these two dominant orientations occur in the southwest of the map area where significant dextral faulting occurs (figure 15, subregion 3). No clear or consistent cross cutting relationships between the strike-slip and normal faults was evident.
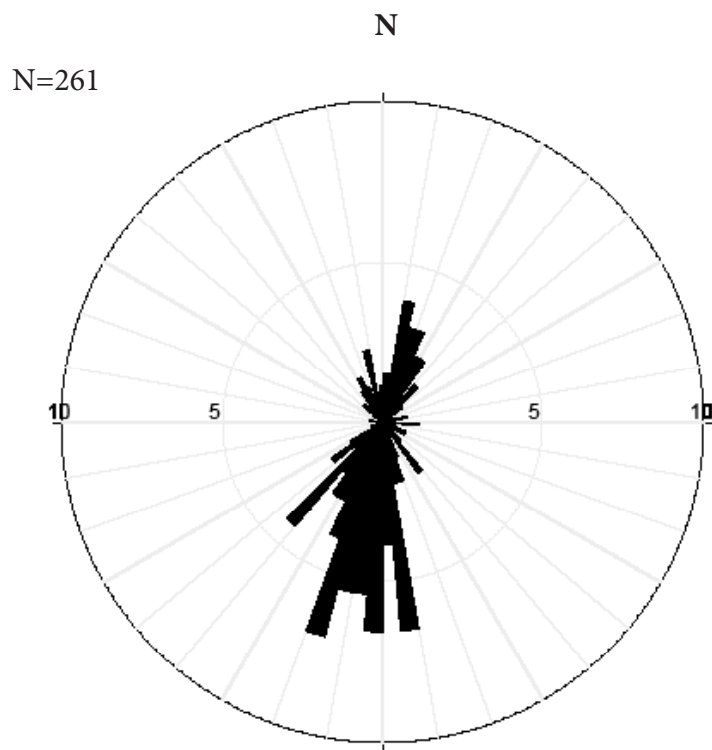

Figure 16. A rose diagram showing all faults recorded in the study showing the frequency of each orientation. A bin size of 5° is used. The right hand rule is used meaning, the strike of each fault is based on its dip *e.g.,* a N-S fault dipping west is documented striking 180° while a N-S fault dipping east is 000°.

Tertiary flood basalts in southern Eyjafjörður are cut by numerous steeply dipping N-S faults. Faults are commonly concentrated along dike margins. Slip direction of these faults locally occurs on mineralized surfaces. Faults in the region vary in orientation, offset and slip direction on both an outcrop and regional scale. Commonly both vertical and horizontal slickenlines occur in close proximity to one another.

Deformation in the area is accommodated by numerous small-scale and large-scale faults. A total of 261 unique faults were mapped during this investigation and are classified by their slip line orientation. Of the 261 mapped faults 204 contain the kinematic indicators necessary to determine sense of slip on the faults, such as the presence of Riedel shears or other shear-sense indicators and a clear slickenline orientation. Of the 204 faults used in the kinematic analysis of the region, 140 (68.6%) are strike-slip, with striae orientations from 0°-30° from horizontal. Of the total faults, 64 (31.4%) had striae rakes greater than 30° (31°-90°) and were mapped as normal faults. The average strike of normal faults is 003° (no reverse faults were observed in this investigation) (figure 17). Sinistral faults make up 104 of the 140 strike-slip faults. Sinistral faults are the dominate style of faulting and are widely distributed throughout the mapping area, sinistral faults have an average strike of ~005°. Only 36 dextral faults were observed. These faults were concentrated in the southwestern portion of the map area and have an average strike of 031°. Dextral faults are observed sporadically throughout and generally had a more NW strike relative to the dominant sinistral faults. Both sinistral and normal faults commonly occur in close proximity to one another on nearly parallel planes.
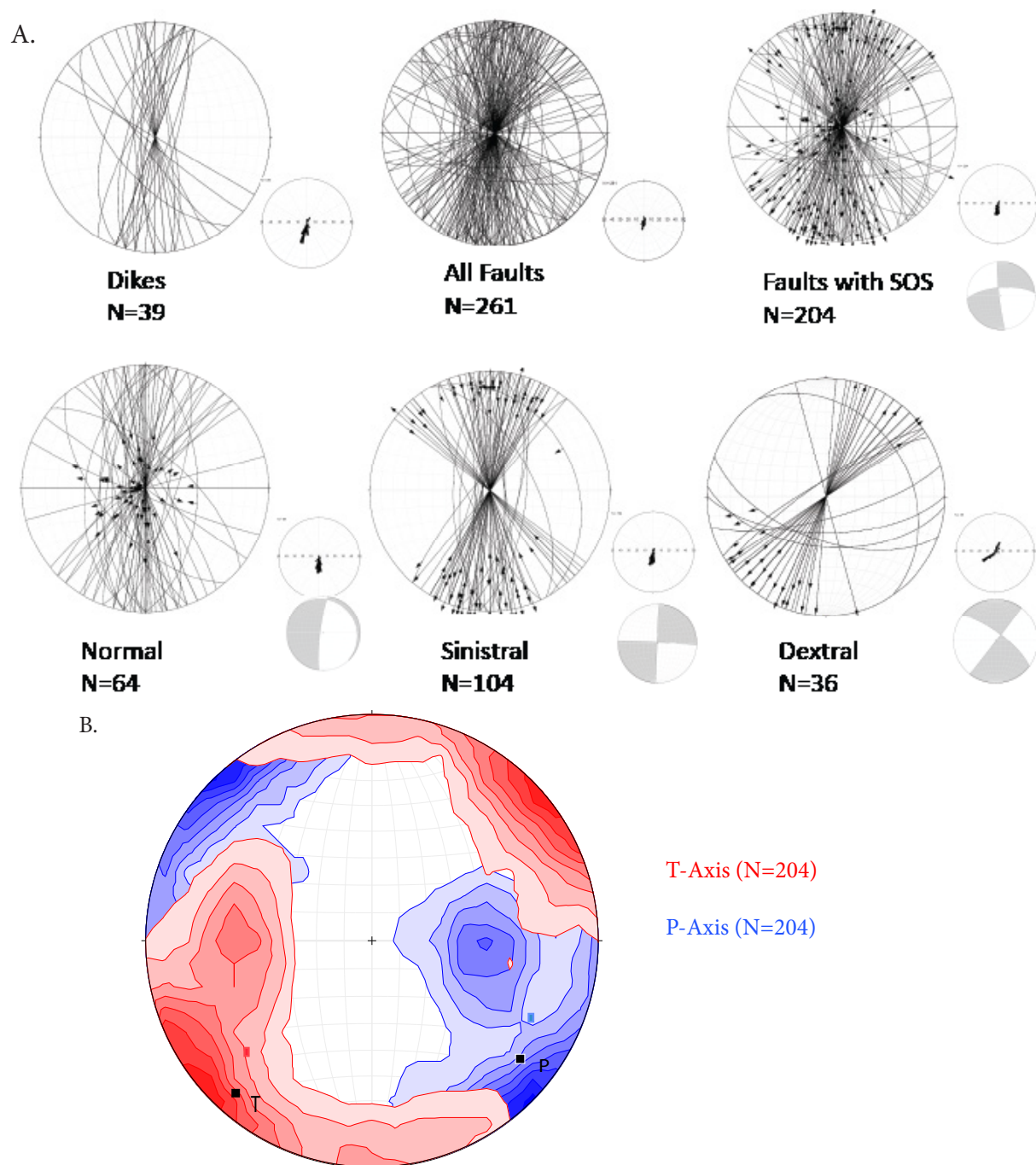
Figure 17. Fault and dike measurements are grouped based on their attributes (see text for definitions). **A.** Great circles-the orientation of the mapped features (lower hemisphere stereographic projection) with the hanging wall slip direction where determined. Rose diagrams show frequency of trends. **B.** Lower hemisphere stereographic projection of contoured P and T axes, using the Kamb contouring method (Kamb, 1959).

Although strike-slip and normal faults occur in close proximity and similar orientation, strike-slip faults have a higher frequency and broader geographic distribution than normal faults. Normal fault trends in the area are highly variable; but overall there is a ~N-S preferred orientation. No significant cluster (more than 5 measurements in a 10° range) of normal faults exist outside of the 325°-035° range. Although strike-slip faults appear to have the same dominant N-S orientation overall, there are two distinct clusters of strike-slip faults at 310-320° and 040°-050° range. The NW, 310-320° cluster is a group of widely dispersed sinistral-slip faults observed in subareas: 1,7,8,12,14. The NE, 040°-050° cluster appears to be a dextral-slip zone and
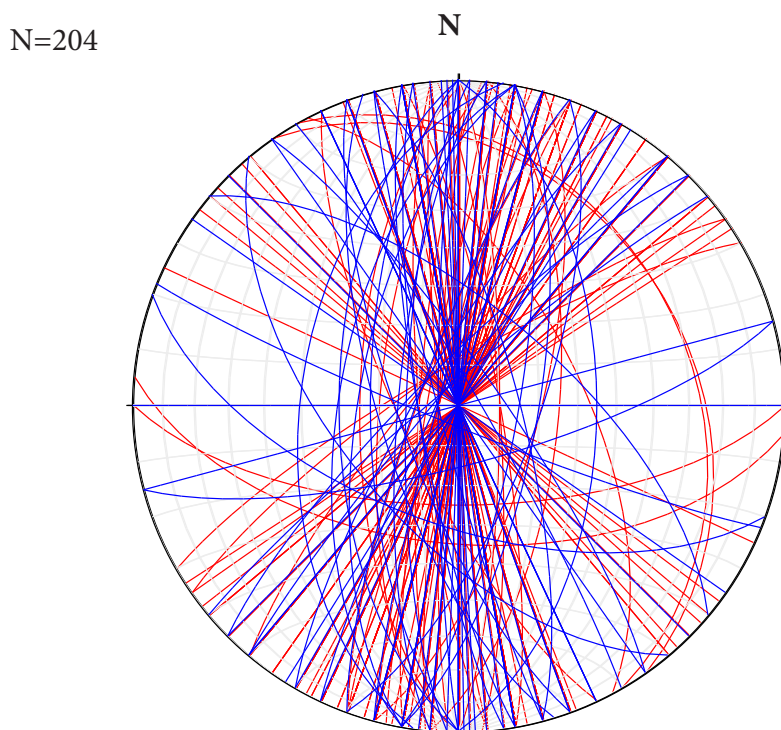
Figure 18. Total population of the 204 fault measurements with sense of slip that includes normal and strike-slip faults. Fault planes projected in a lower hemisphere stereographic projection, The blue planes - striae rakes >30°, red fault planes - striae rakes are ≤30°

is concentrated to subarea 3. Subarea 3 or the Syðragil Quarry, seems to be the only dominantly dextral-slip area observed in this study.

Large outcrops, showing significant evidence of faulting demonstrate patterns, of closely spaced, high-angle and low-angle slip indicators. The clearest examples of bimodal distribution of normal and strike-slip faults with similar orientations is in areas with particularly high densities
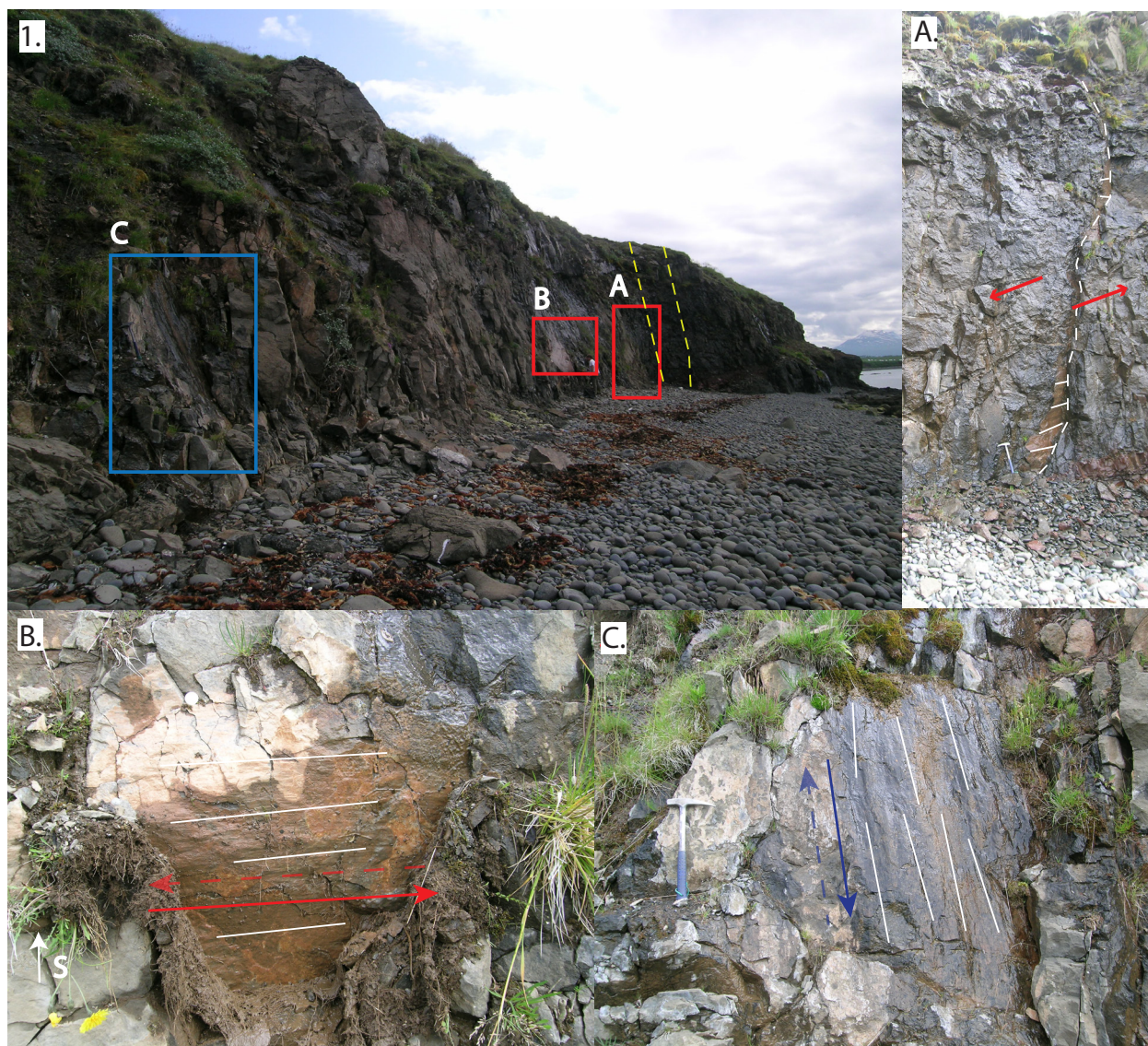
Figure 19. Normal and strike-slip faults in the same outcrop (figure 15, subarea #6). **A**) Fault plane with nearly horizontal slickenlines on a sinistral strike-slip fault. The normal and sinistral faults occur within 10-15 m. **B**) Low angle slickenlines on a sinistral strike-slip fault. **C**) Purely dip-slip normal fault surface with clear sub-vertical striations.

of faulting (*e.g.* subarea 6) (figures 13 and 16). Areas of high density faulting such as subarea 6 occur along dike margins where the dike has been eroded or excavated leaving the fault surfaces exposed.

Outcrops with a high density of faults (figure 19) display well preserved slickensided surfaces as well as kinematic indicators necessary to determine the sense of shear on a fault plane. Outcrops displaying closely spaced, similarly oriented fault planes are an ideal place to identify any

Syðragil Quarry
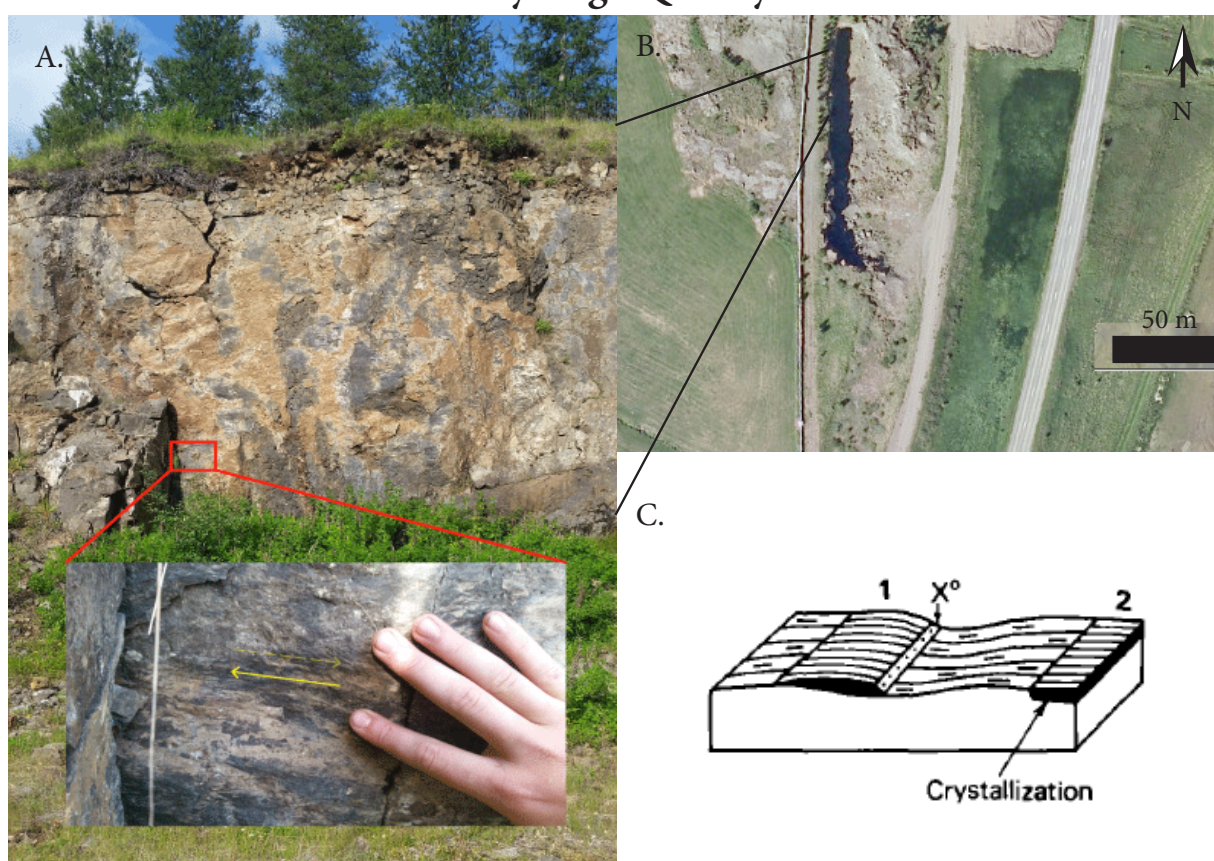
Figure 20. A) Large striated surface displaying characteristic mineral steps that form on the lee side of the asperities (Right-lateral slip). Slickenline orientation ~10° north plunge. B) Areal image of the quarry C) Figure from (Petit, 1897) demonstrating the mineral formation associated with slip on the fault taking place in Fig. 18A (Petit, 1987)

crosscutting relationships between the two sets of normal and sinistral-slip faults. However no clear, consistent crosscutting relationships were determined of the diverse outcrops.

The Syðragil Quarry dextral fault zone lies in the SW of the mapping area (just west of the airport), shown in Figure 15 as subregion #3. This large fault surface on the W wall of the quarry represents the margin of an 0.75 m excavated dike, which extends past the north and south ends of the quarry. Both orientation and sense of slip of the fault are not consistent with the broader observations of this study. The dike remnant visible at the north end of the quarry is faulted suggesting the dike predates the deformational event. The quarry wall is dominated by one large steeply dipping fault plane with excellent sense of shear, indicators (figure 20 B). This fault zone has an average strike of ~030°, kinematic indicators shows dextral strike-slip on an extensive polished fault surface. High-angle normal faults do not occur in this area, the rake of the slickenlines locally reach a maximum of 50° from horizontal. The majority of the faults fell within the strike-slip range (23 of 28 faults). The dextral sense of shear is clearly evident at this outcrop, demonstrating the characteristic mineral step on the fault surface. The mineralized surface is likely composed of clay minerals and iron oxide (Passerini *et al.*, 1997).
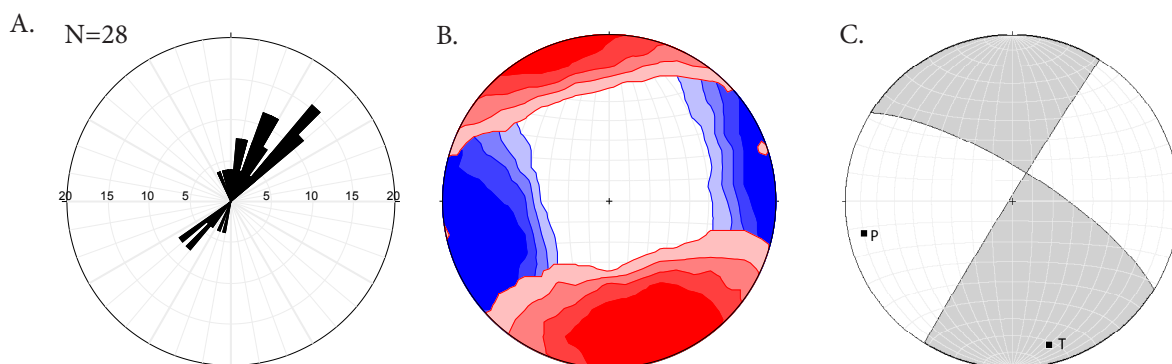
Figure 21. A) Rose diagram showing the frequency of fault orientations recorded in the quarry (right-hand rule applied). B) is a contour of the orientation of the principal strain axes of the 28 fault measurements; using the Kamb contour interval of 2 per 3 significance level; Red T-axes' contours, and blue the P-axes' contours (Kamb, 1959). C) The total strain diagram of the quarry where the shaded area represents the T quadrants and white represents the P quadrants.

4. Interpretation:

4.1. Dikes:

Dike orientation's are more or less consistent throughout the region, varying little over the large area mapped in this study. This consistency suggests the dikes are related, and correspond to a E-W rifting event. The dikes appear to have been injected into flat-lying lava flows, based on their perpendicular relationship. Nearly all dikes observed are highly fractured suggesting they have undergone a great deal of deformation by the faults that cut them (figure 9 and 10). Strike-slip and normal faulting is concentrated along these dike margins. The strain regime has changed between dike injection to strike-slip faulting. Tectonic regime for extension and dike intrusion is incompatible with later strike-slip faulting: dikes appear to be injected when the principal elongation direction (ε_1) was oriented in an ~E-W direction, while the abundance of strike-slip faulting requires a previously unrecognized clockwise rotational component with ε_1 oriented to the NE-SW.

4.2 Faulting:

Sinistral strike-slip faulting is the dominant style of deformation in the area; however, normal-slip and dextral-slip faults are also observed in Southern Eyjafjörður. By compiling the 204 measured faults with sense of shear, a total strain analysis using the 204 P and T axes was conducted, using Faultkin's "Linked Bingham" fault plane solution (Allmendinger, 2012). The orientations derived from the fault plane solution is 356.2^{0} (~N-S). This single orientation is not completely representative of the total data set however. Slip occurs on a wide range of styles and orientations. Normal and strike-slip faults have a bimodal orientation distribution; ~010° (NE) and ~340° (NW) (figure 15). These NE and NW orientations make up nearly ~80% of the total faults used in the strain analysis. The NNE ~010° orientation is sub-parallel to the ~008° trending Northern Rift Zone (Einarsson, 2008), ~50 km east of the eastern boundary of the study area. The distribution and orientation of normal, dextral and sinistral-slip faults observed in Southern Eyjafjörður,

indicates a transtensional setting; encompassing strike-slip and perpendicular extension (Fossen, 1994). In the transtensional model shown in Figure 20, dikes, normal and sinistral strike-slip faulting occurs predominantly in the N-S direction (roughly parallel to the NRZ).
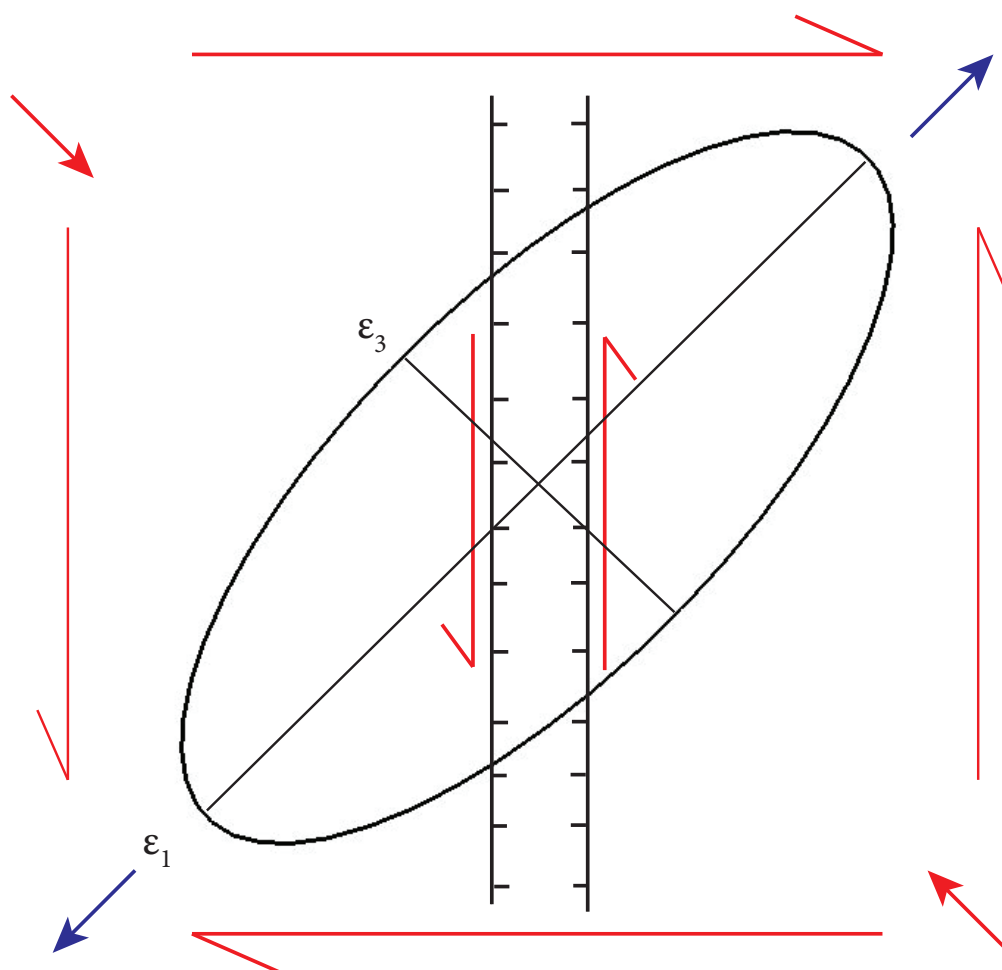
Figure 22. Transtensional setting, where strike slip faults intruding dikes and normal faults. The principal elongation direction ε_1 oriented NE-SW, principle shortening direction ε_3 oriented NW-SE. Results in ~N-S strike-slip faults cutting ~N-S dikes.

5.3 Fault Displacements:

The total displacement of a fault can be estimated using the relationship between total damage zone width to displacement (Faulkner *et al.*, 2011) (figure 24). The relationship between displacement is roughly linear, one to one from damage zones whose width is less than 100 m (Chester et al., 2005 ; Faulkner *et al.*, 2011, Allmendinger et al., 1989, Shipton and Cowie, 2002, Savage and Brodsky 2011) (figure 24).

Significant thickness of fault gouge does not appear to be associated with fault deformation in this area. Damage zones, however, are quite prevalent, where areas that display a high density of fractured rock are associated with slip on fault surfaces (figure 23). Damage zone thickness is not uniform throughout the area, and ranges from meters to nearly 100 m (observed in subarea #15) of meters in thickness. An average damage zone thickness of ~9 m was used to estimate regional strain. This is a rather conservative estimate as total damage zones are not entirely exposed. The value of ~10 m displacement however seems to be in line with observed total offset in the area recorded by Långbacka and Gudmundsson (1995); where an estimate 15 m of offset based on lateral offset of dikes in southern Tröllaskagi. However the total offset of many of these faults could in fact be much larger however. Larger damage zones were observed in stream cuts which cut perpendicular to strike of the faults. The total number of fault data collected from these stream cuts was limited, biasing the damage zone thicknesses to smaller thickness observed on cuts parallel to strike where damages zones have been weathered away or obscured by overgrowth.

Figure 23. A damage zone, with a high fracture density, taken from subarea #1 (figure 15) where sinistral-slip occurs. The total damage zone width at this outcrop is ~10 m in width, indicative of a ~10 m offset.

Figure 24. Scaling relationship between "Damage Zone Width" and total displacement (in a brittle regime)along fault zones for halo zone width is defined in this study as a "micro-fracture damage zone" (Faulkner *et al.*, 2011). Dashed lines represent the range of damage zones thickness; max of ~100 m, minimum of ~1 m, average of 9 m Red highlighted section denotes typical damage zone widths in southern Eyjafjörður.
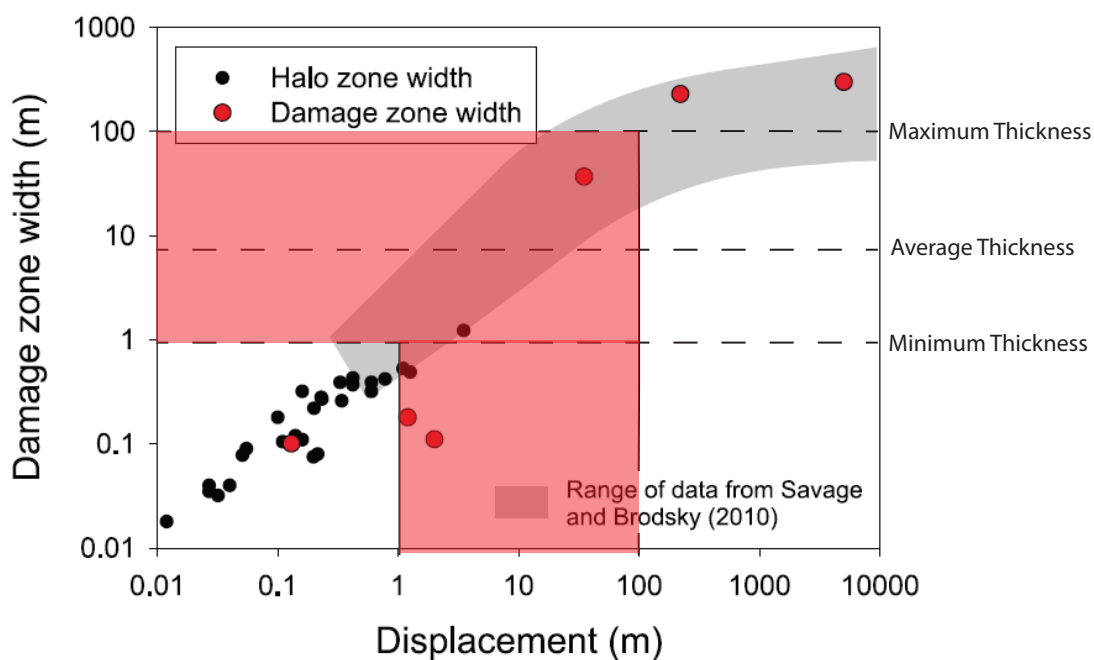
5. Discussion:

Based on the simplified model of rifting, ridge parallel strike-slip faults should not occur outside of a transform zone. Small populations of normal faults, related to tectonic extension have been described as the dominant style of deformation in the region (*e.g.* Jancin ,2010; Långbacka and Gudmundsson, 1995; Hjatarson and Harðardóttir, 2004). The 261 faults show this is not the case. There is a significant population of N-S trending, low-angle sinistral-slip faults. In regard to tectonics, the rift parallel strike-slip faults and related clockwise rotation of crustal blocks is currently unaccounted for. In order to explain these enigmatic ridge-parallel strike-slip faults, it is necessary to evaluate the regional tectonics and how it relates to the broader tectonic context of rifting/spreading in Iceland. There are multiple possible explanations to be discussed below that fit the observations of this study into a broader tectonic context by evaluating other areas where strike-slip faults have been recorded, such as transform zones connecting ridge segments, oblique rifts. It is also important to consider how ridge propagation and proximity to transform systems may affect structures in the region.

5.1. Oblique spreading?

Ridge-parallel strike-slip faults are commonly associated with oblique spreading of rift segments, such as in the Reykjanes ridge in southern Iceland. In the Reykjanes ridge the partitioning of strain is manifested by 30% strike-slip faulting Currently the NRZ is oriented 008°(Einersson, 2008) and the spreading direction is 104.5° at a rate of 18 mm/a (DeMets *et al.*, 2010) (figure 25). The average recorded strike of dikes are ~010°. Because dikes form perpendicular to the direction of spreading the orientation of the rift does not appear to have substantially changed, since the injection of the dikes. This angle of 6.5° is only 7.22% oblique. The shearing component is far too small to observe the 68% strike-slip faulting measured at in the study area (Passerini, 1996). In addition this shearing vector oriented toward the NE on the western side and to the SW on the eastern side of the rift the would result in a minor dextral-slip component. Even if the rift was

highly oblique, the shearing stress is not oriented properly to cause the sinistral strike-slip that is so widely observed.
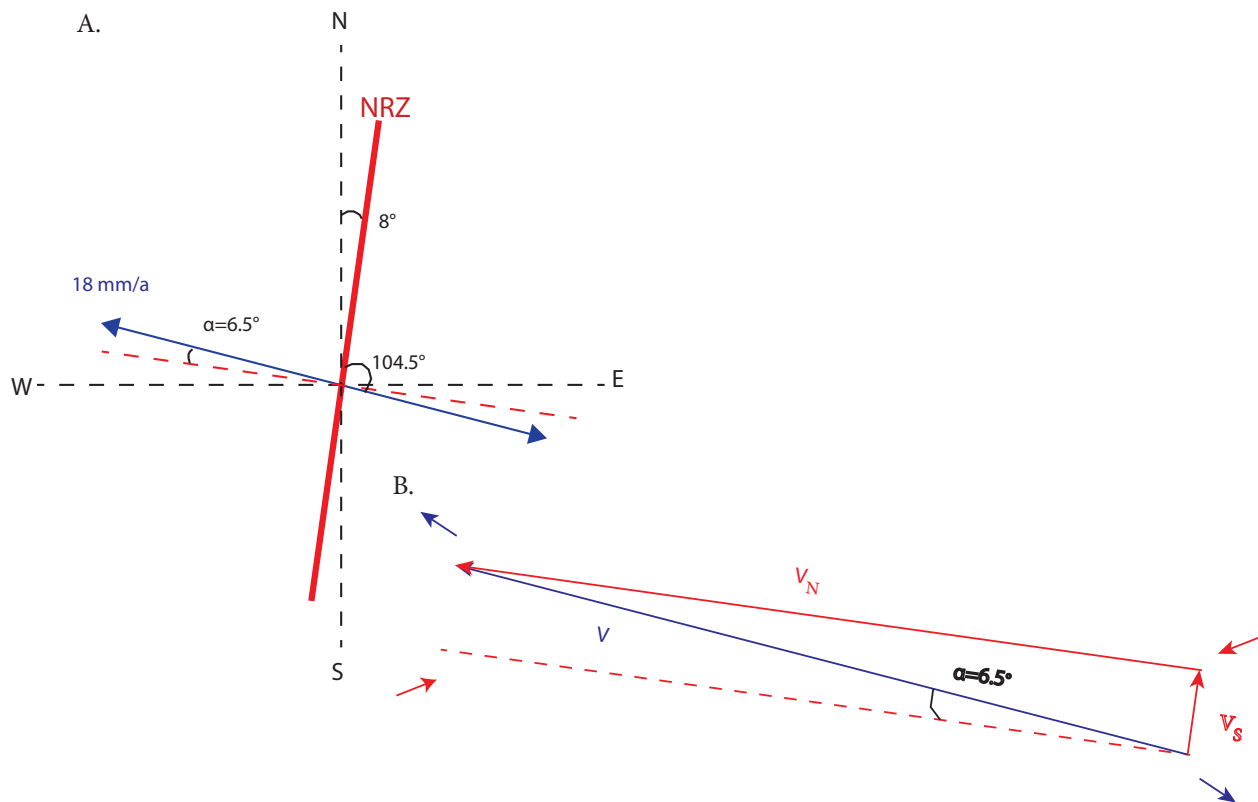
Figure 25. A) Schematic representation of the NRZ's orientation (solid red line) and spreading direction (blue arrows) in northern Iceland: NRZ stikes 008^0 (Einarsson, 2008), current spreading direction of NRZ=104.5^0 at a rate of 18 mm/a(DeMets *et al.*, 2010), obliquity angle (α)=6.5^0 to the NW-SE. Spreading agrees with the average dike orientation. **B)** Spreading vector components: V=total spreading, V_N=velocity of spreading normal to NRZ, V_S= shearing velocity (spreading perpendicular to the ridge). This orientation should result in a minor dextral-slip component subparallel to NRZ.

5.2. Unrecognized Transform?

A previously unrecognized transform segment south of the Davík Liniment could possibly explain the presence of the style of faulting observed in Southern Eyjafjörður. Within the TFZ
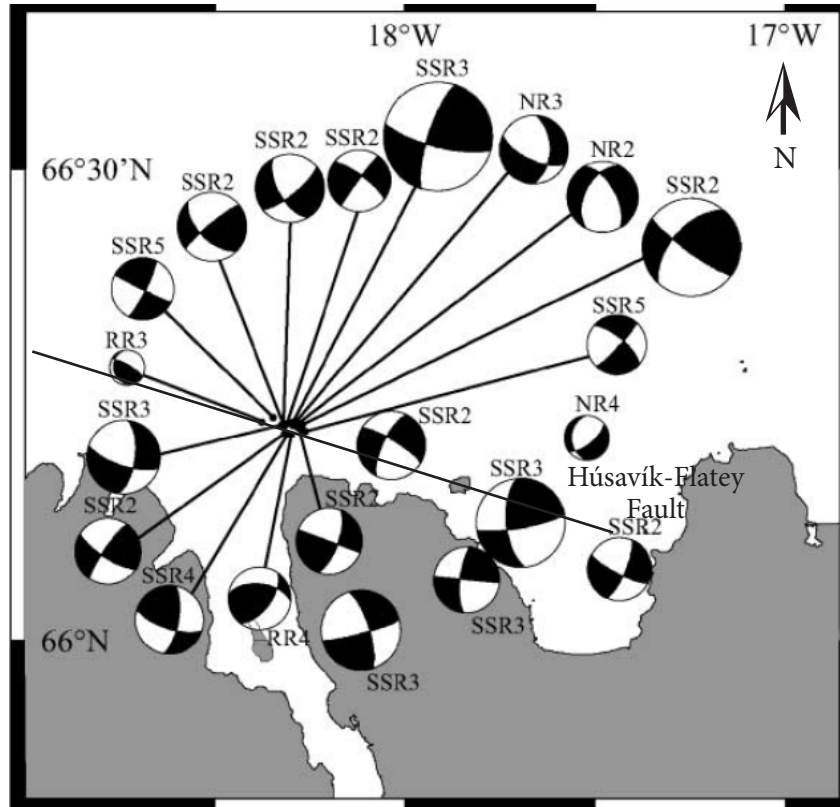
Figure 26. A map of earthquake focal mechanisms from the Húsavík-Flatey fault. The white quadrants represent compression while the black quadrants represent extension, showing dominant left-lateral motion on these faults (modified from Garcia *et al.*, 2002).

dextral-slip is accommodated by perpendicular, *en echelon*, sinistral strike-slip faults (bookshelf faulting). North of the Dalvík lineament in Flateyjarskagi, normal and sinistral-slip faults have been documented striking ~015°, become increasingly rotated to the east northward toward the Húsavík-Flatey Fault, that runs NNW through the northern tip of Flateyjarskagi (Young *et al.*, 1985). The orientation of faults (~N-S, predominately normal and sinistral-slip faults) immediately north of the Dalvík lineament is similar to that observed in southern Eyjafjörður area. These faults with similar orientations are a described as purely extensional structures by
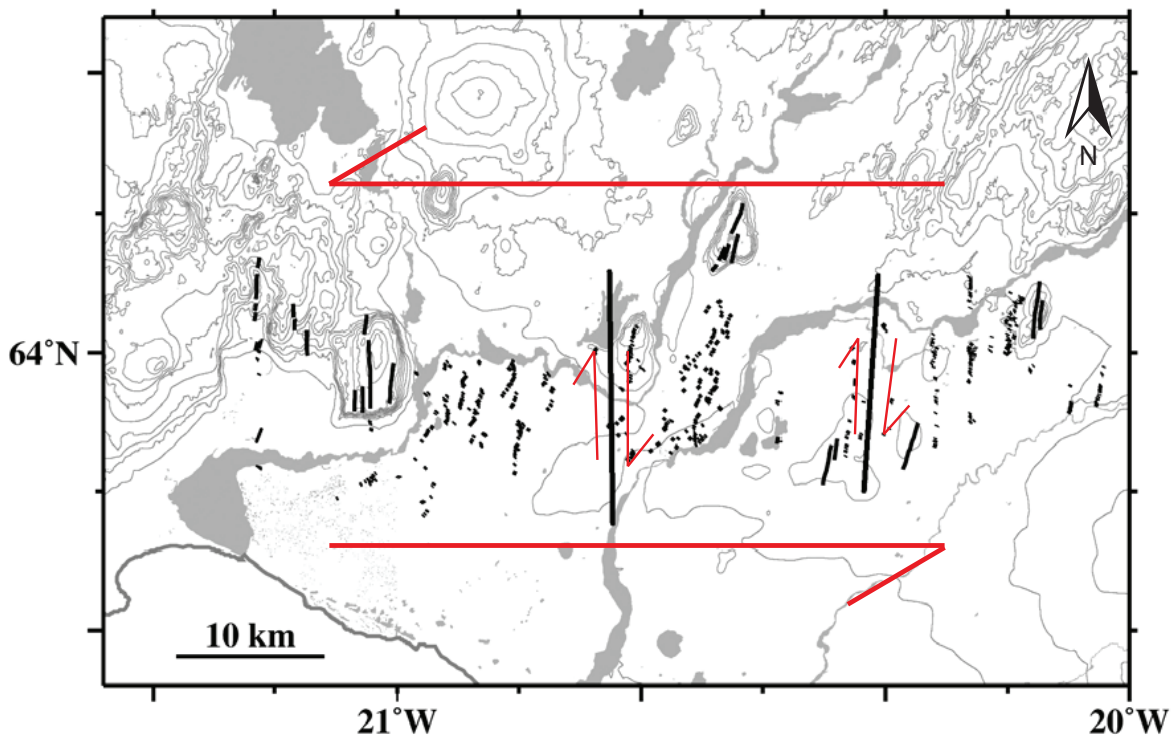
Figure 27. The South Iceland Seismic Zone. Black dots - earthquake epicenters; heavy black lines-mapped fault traces (modified from Einarsson, 2008).

Young *et al.* (1985). In Northern Flateyjarskagi these features are rotated due to the influence of the Húsavík-Flatey fault (Young *et al.*, 1985). Within the transform zones focal mechanisms from faults indicate dominantly sinistral-slip displacement with ~N-S to NE orientations (figure 26). Faulting in these active transform zones is well documented and the style of faulting appears to be analogous to the faults measured in the region investigated. The left step from the NRZ to the Kolbeinsey ridge likely dates back to the initiation of the NRZ/ERZ ~7 ma (*e.g.* Einarsson, 2008; Hackman *et al.*, 1990; Young *et al.*, 1985). It is possible that the transform zone once extended farther south than previously recognized, based on the observations of ridge-parallel strike-slip faults made in this study, south of the Dalvík lineament. If we postulate that the investigated region resembles a transform zone, it is useful to compare it to the more intensely studied and well understood South Iceland Seismic Zone (SISZ) as an analog. The SISZ marks a right step in the plate boundary from the Reykjanes Ridge to the ERZ. Here sinistral-slip is accommodated by bookshelf faulting (a perpendicular series of subparallel dextral strike-slip faults). The subparallel

dextral-slip faults are spaced between 1-6 km apart (Bergerat *et al.*, 2011) and their lengths are on average ~7 km with a maximum fault length of 18 km (Einarsson, 2008) (figure 27).

Although the explanation of a unrecognized transform zone, appears to explain the presence of ridge-parallel strike-slip faults in the study area it is not likely. Strike-slip faulting is present over a much longer zone than has been recognized in the SISZ. Faults are observed over the entire 50 km length of the mapping area and do not appear to be constrained to a specific N-S swath as they are in the SISZ or in the TFZ strands (Húsavík-Flatey fault or the Grímsey fault (figures 4, 15 and 26). A transform zone would also feature a defined lineament that cuts the features in the area such as the Dalvík lineament to the north of the mapping area. Features such as dikes and faults that undergo substantial rotation as they approach transform faults such as in northern Flateyjarskagi (Young *et al.*, 1985; Långbacka and Gudmundsson, 1995). Mapped dikes and faults directly the south of the study area seem to have the same orientation as they approach the southern boundary of the area (Garcia *et al.*, 2008). Thus it is unlikely that the TFZ extends south past the Dalvík lineament based on the lack of any recognizable features cutting the area, the broad N-S occurrence of the strike-slip faults and the lack of rotation of features to the south.

5.3. Influences of Ridge Propagation?

Rift propagation along spreading centers is a well documented phenomena where differential spreading rates is observed along divergent boundaries. This model of propagating rift where the lengthening segment of the active rift gradually supplants spreading of dying rift. As the active rift propagates, the spreading rate increases from zero at the propagator tip, to the maximum spreading rate at the oldest portion of the rift. As a result of these different rates new lithosphere is created faster at the older part of the rift and progressively slower as you travel up the ridge towards the propagator tip. This creates a wedged-shaped geometry of new lithosphere bound by pseudo-faults on either side (Hey, 2004; Karson *et al.*, 2011) (figure 28). This differential spreading causes mircoplate rotation on either side of the rift where small parts of the lithosphere has its own pole of rotation independent of the two rifting plates. This microplate rotation due to

propagating rifts is observed in both continental and oceanic spreading centers and is expensively studied in the East Pacific Rise and East African Rift in the Galapagos and Afar respectively (Hey, 2004; Muluneh *et al.*, 2013).

This mircoplate rotation model of can also be applied to rift propagation in Iceland. Spreading rates along both the ERZ and NRZ demonstrate this same behavior of differential spreading rates from the Iceland hotspot to the propagator tips of the ERZ and NRZ (LaFemina *et al.*, 2005).
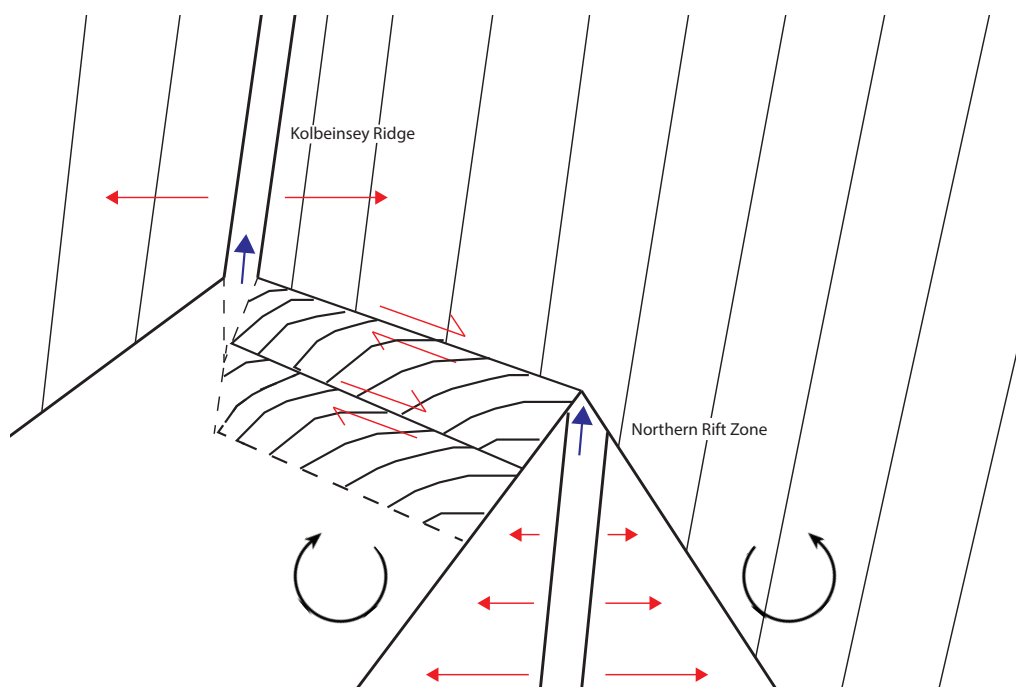
Figure 28. A simplified model of spreading in northern Iceland. Showing The NRZ propagating northward and replacing spreading of the receding Kolbeinsey Ridge, connected by a northerly migrating transform segment. The red arrows indicate relative spreading direction and the blue arrows indicate rift propagation (Karson *et al.,* 2011).

The cause of these propagating rifts in Iceland occurs as a result of the NW migration of the Eurasian-North American plate boundary relative to the Iceland hotspot, where an easterly ridge "jump" occurred approximately 7 Ma, relocating the plate boundary to the Iceland hotspot (*e.g.* , Einarsson, 2008; LaFemina *et al.*, 2005; Young *et al.*, 1985). The NRZ and the ERZ slowly began to supplant the WRZ (in the south) and the Skagafjörður Paleo-Rift (in the north); spreading has
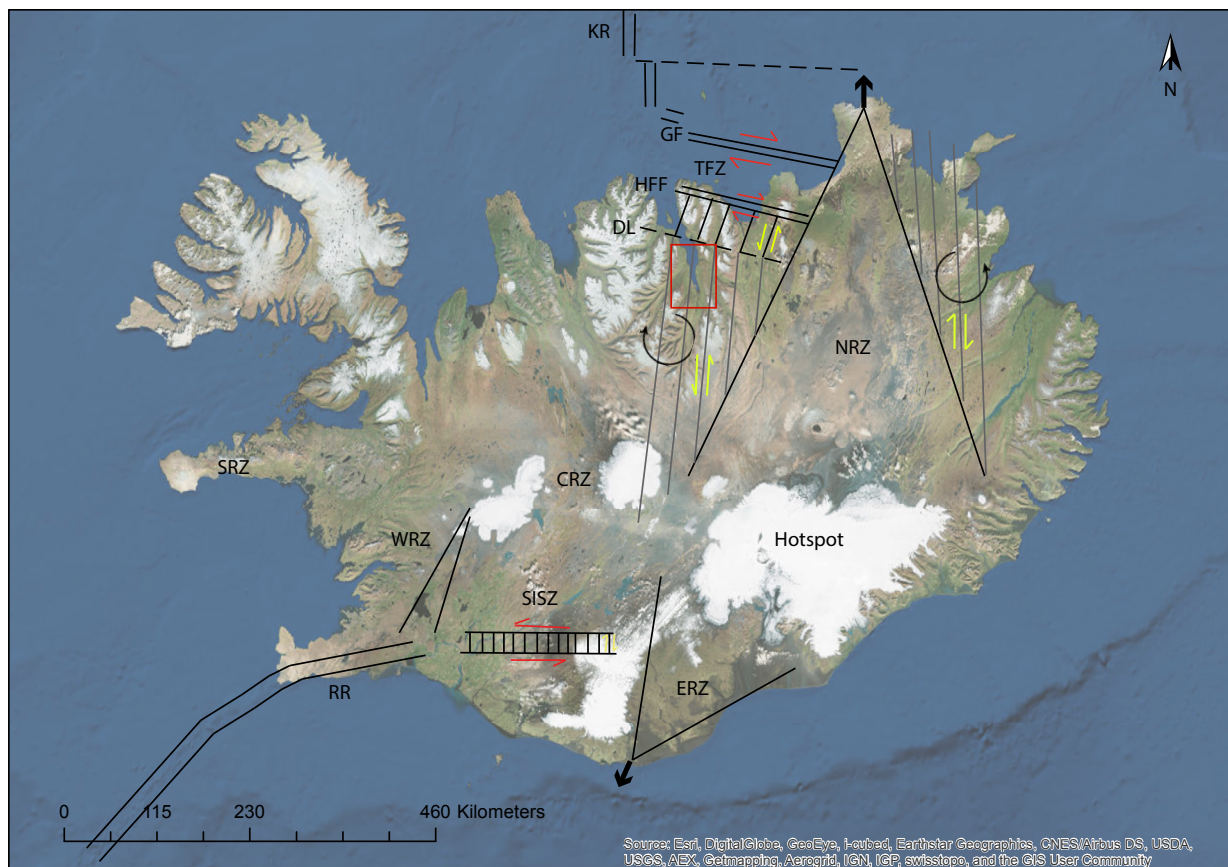
Figure 29. Model of rifting in Iceland: Two most active segments in terms of spreading and volcanism: NRZ and Eastern Rift Zone (ERZ). As the NRZ and ERZ propagate away from the hotspot to the north and south in a v shape bound by pseudo-faults on either side. The spreading rate is greater closer to the hotspot and lowest at the propagator tip causing block rotation manifest by large scale bookshelf faulting and resultant strike-slip faulting (gray lines) (Karson *et al.*, 2011). **1)** Resultant style of deformation in Southern Eyjafjörður (bookshelf faulting) (Red box).
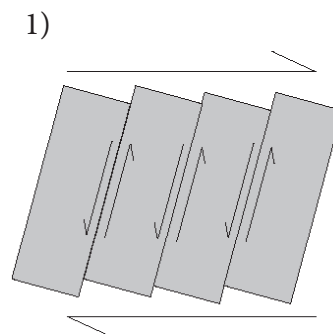
since ceased in the Skagafjörður Paleo-Rift and the NRZ now accounts for the total spreading in Northern Iceland. Differential spreading associated with a northward propagating rift causes a rotational component on either sides of the rift (clockwise and counter clockwise to the east and west respectively). This rotation of the crust is manifest by large scale block rotation of

coherent crustal blocks or "mircoplates" (Hey, 2004; Karson *et al.*, 2011; Muluneh, *et al.*, 2013). This rotation of the crust, is accommodated by large scale bookshelf faulting; such as observed on a smaller scale within individual transform zone such as the SISZ. This large scale bookshelf faulting would result in a wide distribution of km-scale ridge-parallel strike-slip faults with large displacements. In Southern Eyjafjörður ~50 km west of the western pseudo-fault of the NRZ, clockwise rotation would be observed causing a ~E-W dextral shearing component to the lithosphere accommodated by ~N-S sinistral-slip faults such as the ones observed in this study (figure 29).

6. Conclusions:

The Southern Eyjafjörður area, in northern Iceland has enigmatic ridge-parallel strike-slip faults. A kinematic analysis of mainly steeply dipping N-S fault zones in the area reveals predominantly sinistral strike-slip and normal-slip on these fault surfaces. Faults occur primarily along or parallel to dike margins, slip likely occurs preferentially on these weak planes, fault deformation predates the dike intrusions. There is a bimodal distribution of NW and NE fault orientations. Both of these sets include normal and strike-slip faults. No consistent age relationship was determined between the two sets. Based on their similar orientations and kinematics these strike-slip faults likely occurred under similar, if not the same conditions and are superimposed on spreading related normal faults. Faults in the area have particularly clear kinematic indicators, providing unambiguous evidence of transtensional shear throughout the region. Conjugate NE dextral and NW sinistral faults suggest a secondary N-S extension/E-W shortening component to the regional deformation.

The length of these rift-parallel strike-slip faults range from 10-40 km; a number inferred by the fault's kinematic consistency, geographic proximity and inferred displacement. The total

displacement on these faults is inferred based on fault zone scale relationship in a brittle regime, providing ranges between 10 and 100 meters. The deformation in this area can be best explained by large-scale bookshelf faulting, or block rotation. The rotation of crustal blocks may be due to the differential spreading along the northward propagating NRZ. In order to accommodate this rotation, ridge-parallel, structures associated with rifting such as normal faults and dikes are reactivated as N-S sinistral strike-slip faults.

The presence of such large strike-slip faults outside of a transform zone, suggests the current model of rifting in Iceland needs to be reassessed. This phenomena of rift-parallel strike-slip faulting does not appear to be limited to southern Eyjafjörður. Studies with a broad geographic distribution within Iceland such as, Gljúfurá, Kárahnjúkar, Lagarfljót, seem to display similar styles of deformation. The implications of these ridge-parallel strike-slip faults may give insight into how rift propagation impacts the behavior of mid-ocean ridges globally, furthering our understanding of the seafloor.

Appendix

Appendix A

Fault and Dike Measurements

	Way Point	Strike	Dip	Rake					
D	5	190	90		F	19	15	90	5
D	6	350	77		F	19	345	90	5
D	9	200	55		F	19	20	90	-20
D	10	210	75		F	20	340	90	-20
D	11	130	85		F	21	345	75	-85
D	12	175	75		F	24	210	80	120
D	13	195	85		F	27	210	90	20
D	14	120	90		F	27	210	90	-30
D	33	160	90		F	27	180	90	45
D	34	10	90		F	27	215	90	-20
D	17	180	90		F	27	170	90	0
D	22	140	60		F	27	140	90	10
D	23	170	90		F	28	170	80	90
D	25	195	90		F	28	165	85	90
D	27	190	80		F	28	170	90	90
D	36	145	80		F	28	182	77	90
D	15	0	90		F	28	178	90	90
D	15	20	90		F	28	190	68	90
D	8	65	90		F	28	200	90	-12
D	38	170	90		F	28	180	90	0
D	39	190	90		F	28	185	90	10
D	40	200	90		F	28	20	90	25
D	40	200	90		F	28	330	30	90
D	42	175	90		F	28	220	90	70
D	43	200	90		F	29	185	90	40
D	46	185	90		F	29	140	75	-120
D	46	200	90		F	29	220	90	90
D	47	165	90		F	29	215	90	90
D	48	152	90		F	29	195	80	-120
D	51	175	90		F	29	173	90	20
D	52	20	90		F	30	175	90	-10
D	58	180	80		F	30	180	85	90
D	59	190	85		F	30	170	90	90
D	62	195	75		F	30	165	90	0
D	66	20	80		F	30	180	90	-5
D	67	15	75		F	24	200	80	-100
D	71	352	80		F	24	170	90	20
D	58	180	80		F	24	195	90	20
F	15	140	60	-70	F	24	180	90	10
F	15	15	70	0	F	32	190	90	-20
F	19	30	90	20	F	32	225	90	160
					F	32	230	90	150

F	32	220	90	180		F	5	95	55	-145
F	32	20	90	-155		F	5	112	85	-135
F	32	30	90	-160		F	5	180	68	-95
F	32	25	90	-160		F	5	200	80	-27
F	32	40	90	-170		F	5	200	85	-30
F	32	45	90	-165		F	5	220	80	-20
F	32	25	90	-160		F	5	195	90	-10
F	32	10	90	-150		F	5	197	90	0
F	32	17	90	-150		F	5	175	90	0
F	32	345	90	-175		F	5	207	90	10
F	33	170	90	-80		F	5	205	90	12
F	33	160	90	-75		F	5	190	90	0
F	34	12	90	8 S		F	28	325	30	90
F	34	345	90	10 S		F	28	181	65	10
F	34	15	90	15 N		F	28	185	70	10
F	34	40	90	0		F	28	0	55	80
F	34	15	90	5 S		F	15	345	85	0
F	34	5	90	0		F	15	335	90	5
F	34	0	90	0		F	15	17	80	0
F	34	340	90	10		F	15	24	90	15 N
F	35	205	90	-20		F	15	310	90	0
F	35	185	90	-10		F	15	325	90	35
F	35	180	90	30		F	15	315	90	40
F	35	175	90	10		F	15	335	90	35
F	37	155	90	-120		F	15	310	65	65
F	37	172	90	-105		F	15	10	75	-80
F	37	305	90	-100		F	15	20	70	90
F	37	215	90	-160		F	15	332	60	-17
F	27	195	90	20		F	8	20	80	10
F	27	200	90	30		F	8	10	90	-80
F	27	210	90	20		F	8	190	80	90
F	27	180	90	-30		F	8	70	90	0
F	27	180	90	-45		F	8	275	45	45
F	27	215	90	20		F	8	220	70	17
F	27	140	90	10		F	8	250	80	25
F	27	170	90	0		F	8	200	25	15
F	27	190	65	-90		F	41	190	60	90
F	27	32	90	-80		F	42	195	85	-85
F	28	160	90	90		F	44	155	75	10
F	28	195	90	90		F	45	205	90	15
F	28	180	60	80		F	45	210	90	10
F	5	90	65	-155		F	45	200	90	15
F	5	75	75	-135		F	45	135	90	20
F	5	110	60	-130		F	45	240	80	170
F	5	188	50	90		F	45	235	80	170

F	46	357	90	0	F	60	195	90	-15
F	50	190	90	20	F	60	190	90	-20
F	50	170	90	5	F	60	4	90	45 N
F	50	195	90	-5	F	60	90	90	80
F	53	185	90	-80	F	60	200	90	-170
F	54	180	90	80	F	60	170	90	85
F	54	195	90	80 N	F	61	45	90	20 S
F	54	10	90	35 N	F	61	30	90	30
F	54	140	80	10 S	F	61	356	80	10
F	55	10	90		F	61	360	80	30
F	55	40	90	20 E	F	61	350	80	20
F	59	186	85	5	F	61	170	90	10
F	59	184	80	10	F	62	220	90	-165
F	59	190	90	0	F	62	75	90	80
F	59	175	85	15	F	62	190	90	-120
F	59	165	90	50	F	63	28	90	15
F	59	325	80	-70	F	63	220	90	-10
F	59	330	85	-75	F	63	195	90	-10
F	59	230	85	-60	F	64			
F	59	225	80	-60	F	65	25	90	-30
F	59	220	85	-50	F	65	195	90	-75
F	59	187	90	-75	F	66	195	85	-15
F	59	205	90	-80	F	67	15	90	15
F	59	179	90	-70	F	67	170	90	5
F	59	25	80	15 N	F	67	5	65	30
F	59	18	90	5 N	F	67	10	70	40
F	59	20	80	80	F	68	190	82	0
F	59	10	85	80	F	68	185	90	20
F	59	330	90	80	F	69	182	85	5
F	59	30	90	60	F	69	193	85	0
F	59	50	90	70	F	69	178	90	10
F	59	220	90	-20	F	32	230	90	170
F	59	210	90	-50	F	32	215	90	165
F	59	30	90	-10	F	32	220	90	145
F	59	345	90	10	F	32	200	90	180
F	59	10	90	10	F	32	25	90	-175
F	60	9	80	-50	F	32	335	90	-135
F	60	189	90	0	F	32	22	90	-170
F	60	195	90	-10	F	32	12	90	-170
F	60	50	90	10 N	F	32	40	90	-155
F	60	115	90	45 W	F	32	5	90	-170
F	60	90	90	10 E	F	32	0	90	40
F	60	80	90	80 E	F	32	350	90	30
F	60	190	90	-100	F	32	357	90	50
F	60	220	90	30 S	F	72	185	75	-100

F	72	225	90	80
F	72	195	90	0
F	72	202	90	0
F	72	170	90	10
F	72	168	90	0
F	72	175	80	-30
F	70	159	90	0
F	70	172	90	-10
F	70	165	90	5
F	70	175	90	5
F	70	180	90	0
F	70	160	90	-10
F	70	187	90	0
F	70	207	90	-5
F	70	187	90	-10
F	7	160	75	-90
F	7	163	70	-80
F	7	172	80	-85
F	7	195	90	-170
F	7	175	90	-70
F	7	205	85	-90
F	7	190	90	-85
F	7	185	90	-90
F	7	195	90	-90
F	7	182	90	-80
F	71	115	90	0
F	71	170	90	-80
F	71	195	90	15
F	75	132	90	10
F	75	138	90	10
F	75	127	90	15
F	75	235	90	180
F	75	230	90	185
F	75	237	90	180
F	75	232	90	185
F	24	210	90	90

References:

Allmendinger, R. W., J. W. Gephart, and R. A. Marrett (1989), Notes on Fault Slip Analysis, Prepared for the Geological Society of America Short Course on"Quantitative Interpretation of Joints and Faults"November 4 & 5, 1989.

Allmendinger, R. W. (2012). FaultKin 7, http://www.geo.cornell.edu/geology/faculty/RWA/programs/faultkin.html.

Bergerat, F., C. Homberg, J. Angelier, and M. Bellou (2011), Surface traces of the Minnivellir, Réttarnes and Tjörvafit seismic faults in the South Iceland Seismic Zone: Segmentation, lengths and magnitude of related earthquakes, Tectonophysics, 498(1-4), 11–26, doi:10.1016/j.tecto.2010.11.014.

Bjarnason, I. Þ. (2008), An Iceland Hotspot Saga, , (58), 3–16.

Brandsdóttir, B., B. Richter, C. Riedel, T. Dahm, G. Helgadóttir, E. Kjartanson, R. Detrick, A. Magnússon, Á.L. Ásgrímsson, B.H. Palsson, J. Karson, K. Sæmundsson, Mayer, B. Calder, and N. Driscoll (2004), Tectonic details of the Tjornes Fracture Zone and onshore-offshore ridge-transform in N-Iceland, EOS, Transactions of the American Geophysical Union, 85, T41A-1172.

Chester, J. S., F. M. Chester, and A. K. Kronenberg (2005), Fracture surface energy of the Punchbowl fault, San Andreas system., Nature, 437(7055), 133–6, doi:10.1038/nature03942.

Chutas, L.A., J. A. Karson, and K. Sæmundsson, (2006), Rift-Parallel Strike Slip Faulting in the Kárahnjúkar area of Eastern Iceland.: American Geophysical Union, Fall Meeting, abstract #T43D-1687.

DeMets, C., R. G. Gordon, and D. F. Argus (2010), Geologically current plate motions, Geophysics. J. Int., 181, 1–80, doi:10.1111/j.1365-246X.2009.04491.x.

Einarsson, P. (2008), Plate boundaries, rifts and transforms in Iceland, Jökull, 58, 35-58.

Faulkner, D. R., T. M. Mitchell, E. Jensen, and J. Cembrano (2011), Scaling of fault damage zones with displacement and the implications for fault growth processes, Journal of Geophysics. Res. Solid Earth, 116(May), 1–11, doi:10.1029/2010JB007788.

Fossen, H., B. Tikoff, and C. Teyssier (1994), Strain modeling of transpressional and transtensional deformation, Nor. Geol. Tidsskr., 74, 134–145.

Garcia, S., J. Angelier, F. Bergerat, and C. Homberg (2002), Tectonic analysis of an oceanic transform fault zone based on fault-slip data and earthquake focal mechanisms: The Húsavík-Flatey Fault zone, Iceland, Tectonophysics, 344, 157–174, doi:10.1016/S0040-1951(01)00282-7.

Garcia, S., J. Angelier, F. Bergerat, C. Homberg, and O. Dauteuil (2008), Influence of rift jump and excess loading on the structural evolution of northern Iceland, Tectonics, 27(1), n/a–n/a, doi:10.1029/2006TC002029.

Gudmundsson, A., and S. Brynjolfsson (1993), Overlapping rift-zone segments and the evolution of the South Iceland Seismic Zone, Geophys. Res. Lett., 20(18), 1903, doi:10.1029/93GL01888.

Hackman, M.C., King, G.C.P., Bilham, R., (1990). The mechanics of the South Iceland Seismic Zone. J. Geophys. Res. 95 (B11), 17,339–17,351.

Hardarson, B. S., J. G. Fitton, R. M. Ellam, and M. S. Pringle (1997), Rift relocation — A geochemical and geochronological investigation of a palaeo-rift in northwest Iceland, Earth Planet. Sci. Lett., 153(97), 181–196, doi:10.1016/S0012-821X(97)00145-3.

Hey, R. N. (2004), Propagating rifts and microplates at mid-ocean ridges. In Selley, R. C. (ed.), Encyclopedia of Geology. London: Academic Press, pp. 396–405.

Hjatarson, Á. (2001), Vaðlaheiði, Jarðfræðikort. Orkustofnun, Reykjavík. Allen, R. M., *et al.*, (2002), Plume-driven pluming and crustal formation in Iceland, Journal of Geophysical Research, vol. 107, no. b8, 10.1029/2001JB000584.

Hjatarson, Á. and V. B. Harðardóttir (2004), Höfðahverfi, Geological Map. ISOR Iceland GeoSurvey, Reykjavík.

Hjatarson, Á. and H. E. Jónsdóttir (2004), Fnjoskadalur, Geological Map, 3. ed. ISOR GeoSurvey, Reykjavík.

Homberg, C., F. Bergerat, J. Angelier, and S. Garcia (2010), Fault interaction and stresses along broad oceanic transform zone: Tjörnes Fracture Zone, north Iceland, Tectonics, 29 (Figure 1), 1–12, doi:10.1029/2008TC002415.

Jancin, M. A. (2010), Volcano-Tectonic Evolution of Flateyjarskagi, North Central Iceland, 1–189 pp., The Pennsylvania State University.

Jóhannesson, Á. and Á. Hjatarson (2003), Hjalteyri, Geological Map. National Energy Authority, Reykjavík.

Jóhannesson, H. and K. Sæmundsson (2009), Geological Map of Iceland institute of Natural History, Reykjavík (1st edition).

Kamb, W. B. (1959), Ice Petrofabric Observations from Blue Glacier, Washington, Relation to Theory and Experiment, J. Geophys. Res., 54(11), 1891–1909.

Karson, J. A., A. J. Horst, and A. F. Nanfito (2011), A New Look at Spreading in Iceland: Propagating Rifts, Migrating Transform Faults, and Microplate Tectonics, Abstract T23D-2429 presented at Eos Transactions of the American Geophysical Union, Fall Meeting Supplement, AGU, San Francisco, Calif., 5-9 Dec.

Kristjansson, L., A. Gudmundsson, and B. S. Hardarson (2004), Stratigraphy and paleomagnetism of a 2.9-km composite lava section in Eyjafjördur, Northern Iceland: A reconnaissance study, Int. J. Earth Sci., 93, 582–595, doi:10.1007/s00531-004-0409-4.

Kumar, P., R. Kind, K. Priestley, and T. Dahl-Jensen (2007), Crustal structure of Iceland and Greenland from receiver function studies, J. Geophys. Res., 112(B3), B03301, doi:10.1029/2005JB003991.

LaFemina, P. C., T. H. Dixon, R. Malservisi, T. Árnadóttir, E. Sturkell, F. Sigmundsson, and P. Einarsson (2005), Geodetic GPS measurements in south Iceland: Strain accumulation and partitioning in a propagating ridge system, J. Geophys. Res., 110(B11), B11405, doi:10.1029/2005JB003675.

Långbacka, B. O., and A. Gudmundsson (1995), Extensional tectonics in the vicinity of a transform fault in north Iceland, Tectonics, 14, 294–306, doi:10.1029/94TC02904.

Lawver, L. A. and R. D. Müller (1994), Iceland Hotspot Track, Geology, 22, 311–314.

Marrett, R., & R. Allmendinger (1990), Kinematic analysis of fault-slip data. Journal of Structural Geology, 12(8), 973–986.

Muluneh, A. A., T. Kidane, J. Rowland, and V. Bachtadse (2013), Counterclockwise block rotation linked to southward propagation and overlap of sub-aerial Red Sea Rift segments, Afar Depression: Insight from paleomagnetism, Tectonophysics, 593, 111–120, doi:10.1016/j.tecto.2013.02.030.

Nanfito, A., J. A. Karson (2009), Complex Rift-Parallel, Strike-Slip Faulting in Iceland: Kinematic Analysis of the Gljúfurá Fault Zone: American Geophysical Union, Fall Meeting, abstract #T21D-1866.

Passerini, P., M. Marcucci, G. Sguazzoni, and E. Pecchioni (1997), Longitudinal strike-slip faults in oceanic rifting: a mesostructural study from western to southeastern Iceland, Tectonophysics, 269(November 1995), 65–89, doi:10.1016/S0040-1951(96)00153-9.

Petit, J. P. (1987), Criteria for the sense of movement on fault surfaces in brittle rocks. Journal of Structural Geology, 9(5/6), 597–608.

Reed, C., (2006), Marine science: Boiling points, Nature, vol. 439, doi:10.1038/439905a.

Savage, H. M., and E. E. Brodsky (2011), Collateral damage: Evolution with displacement of fracture distribution and secondary fault strands in fault damage zones, J. Geophysics. Res. Solid Earth, 116, doi:10.1029/2010JB007665.

Sæmundsson, K., and E. Gunnlaugsson (2002), Icelandic Rocks and Minerals Paperback, Mal Og Menning, Reykjavik.

Sæmundsson, K., J. Karson (2006), Stratigraphy and Tectonics of the Húsavík, Western Tjörnes Area Prepared for Alcoa and HRV Engineering.

Shipton, Z. K., and P. A. Cowie (2003), A conceptual model for the origin of fault damage zone structures in high-porosity sandstone, J. Struct. Geol., 25, 333–344, doi:10.1016/S0191-8141(02)00037-8.

Young, K. D., M. A. Jancin, B. Voight, and N. I. Orkan (1985), Transform Deformation Of Tertiary Rocks Along The Tjornes Fracture Zone, North Central Iceland, Journal Of Geophysical Research, Vol. 90, No. B12, Pages 9986-10,010.

<u>Vita</u>

Name of Author: James Arthur Proett

Place of Birth: Houston, Texas

Date of Birth: January 26, 1990

Undergraduate School Attended:

- Texas A&M University, College Station, Texas